Towards Modelling Locomotion using EMG Informed 3D Models: Application to Cerebral Palsy

M Sartori[1Ψ], J W Fernandez[2,3Ψ], L Modenese[4,5,6], C P Carty[5,6,7], L A Barber[8], K Oberhofer[2], J Zhang[2], G G Handsfield[2], N S Stott[9], T F Besier[2,3], D Farina[10], D G Lloyd[6,7]

Ψ Equal first authors.

1. Klinik für Unfallchirurgie, Orthopädie und Plastische Chirurgie, Institute of Neurorehabilitation Systems, University Medical Center Göttingen, Georg-August University, Göttingen, Germany.
2. Auckland Bioengineering Institute, University of Auckland, New Zealand.
3. Department of Engineering Science, University of Auckland, New Zealand.
4. Department of Mechanical Engineering, The University of Sheffield, UK.
5. Queensland Children's Motion Analysis Service, Queensland Paediatric Rehabilitation Service, Children's Health Queensland, Brisbane, Australia
6. Menzies Health Institute Queensland, Griffith University, QLD, Australia.
7. School of Allied Health Sciences, Griffith University, Queensland, Australia.
8. Queensland Cerebral Palsy and Rehabilitation Research Centre, Child Health Research Centre, Faculty of Medicine, The University of Queensland, Brisbane, Australia.
9. School of Medicine, University of Auckland, New Zealand.
10. Department of Bioengineering, Imperial College London, UK.

Submitted as an invited Journal Article to WIREs Systems Biology and Medicine

Address correspondence to:

Justin Fernandez PhD

Auckland Bioengineering Institute

University of Auckland, New Zealand

Email: j.fernandez@auckland.ac.nz

Phone: +64 9 373 7599 ext 89196

Key words: musculoskeletal; rigid body; continuum 3D models; EMG informed model: Musculoskeletal Atlas Project

Abstract

This position paper proposes a modeling pipeline to develop clinically relevant neuromusculoskeletal models to understand and treat complex neurological disorders. Although applicable to a variety of neurological conditions we provide direct pipeline applicative examples in the context of cerebral palsy (CP). This paper highlights technologies in; (i) Patient-specific segmental rigid body models developed from Magnetic Resonance Imaging for use in inverse kinematics and inverse dynamics pipelines; (ii) Efficient population based approaches to derive skeletal models and muscle origins/insertions that are useful for population statistics and consistent creation of continuum models; (iii) Continuum muscle descriptions to account for complex muscle architecture including spatially varying material properties with muscle wrapping; (iv) Muscle and tendon properties specific to CP; and (v) Neural based electromyography-informed methods for muscle force prediction. This represents a novel modeling pipeline that couples for the first time electromyography extracted features of disrupted neuromuscular behavior with advanced numerical methods for modelling CP-specific musculoskeletal morphology and function. The translation of such pipeline to the clinical level will provide a new class of biomarkers that objectively describe the neuro-musculo-skeletal determinants of pathological locomotion and complement current clinical assessment techniques, which often rely on subjective judgment.

1 Introduction

Cerebral palsy (CP) is an umbrella term for a group of motor impairment disorders caused by a non-progressive lesion in the developing child's brain during pregnancy or shortly after birth.[1] Following the central nervous system lesion the damage to the descending pathways causes (i) paresis, a reduction or failure of voluntary activation and (ii) muscle overactivity, which can be described as spasticity, spastic dystonia and spastic co-contraction[2]. Spasticity, a velocity-dependent increase in muscle tone[3], is the primary sign of spastic-type CP. Spasticity interferes with normal muscle growth[4] resulting in the development of fixed contractures of the muscle-tendon unit leading to muscle weakness and loss of function[5]. While the brain lesion is static, secondary musculoskeletal problems such as reduced joint range of motion, increased joint stiffness, and muscle weakness can progress with age[6, 7]. These impairments contribute to a gradual loss of functional capacity[8], characterized by deterioration in gait and reduced muscular strength throughout adolescence and young adulthood in individuals with spastic-type CP[9].

Orthopedic surgery is a key component in the clinical management of musculoskeletal pathologies in CP. Single- and multi-level surgeries, including muscle-tendon lengthening, tendon transfer and bone derotation osteotomies, are performed to avoid progressive worsening of musculoskeletal impairments, improve gait patterns, and thus, patients' quality of life[10-12]. These treatments are commonly prescribed and performed with no objective understanding of the functional changes expected to occur at the neuro-musculo-skeletal levels post-surgery. Common methods to assess the degree of musculoskeletal pathologies and gait impairments prior to surgery include physical examination, observational analysis of walking and quantitative clinical gait analysis[13]. However, existing assessment techniques rely on subjective judgment[14], do not account for complex muscle and tendon architecture nor do they account for the neural control of muscle during walking. As a consequence,

planning and evaluation of orthopedic surgery in children with CP has remained difficult. There is no agreement on the details of the structural changes that occur secondary to the neurological disorder[15], and evidence for the efficacy of most orthopedic operations remains lacking[10, 12].

Patient-specific neuromusculoskeletal modeling pipelines can provide estimates of internal body variables that would be otherwise difficult to derive experimentally. These may include estimates of the mechanical force produced by muscles and series elastic tendons, their levels of stiffness, the mechanical loads exerted on articular joints, and the final impact on articular range of motion. This would enable objectively quantifying which muscles are too tight (i.e. preventing natural joint motion) or too weak (i.e. causing abnormal joint loads) pre surgery. Similarly, it would enable predicting how muscle and joint function would vary post-surgery (i.e. after muscle-tendon lengthening or tendon transfer), thus personalizing treatments to an individual patient and maximize the subsequent rehabilitation outcome.

Current modeling pipelines characterize either the neural[16, 17] or the mechanical determinants[18] of CP locomotion. This poses a major challenge to the treatment of motor impairment in CP, where disrupted mechanical function (i.e. abnormal joint loading and stiffness) must be understood in the context of its disrupted neural origin (i.e. abnormal neuromuscular function)[19-21]. As a result, despite the understanding of the neural and mechanical processes underlying CP movement, there currently is no relevant knowledge of the neuromechanical interplay and couplings *in vivo* in the intact individual[22].

With this position paper we propose a clinically relevant neuromusculoskeletal modelling pipeline that accounts for both neuromuscular and musculoskeletal properties of an individual patient. Parts of the proposed pipeline can be applied to investigate a variety of neurological conditions (i.e. see Sections 6 and 7). However, with this paper we provide applicative examples in the context of CP and subsequent personalization of

neurorehabilitation interventions[19]. The past decade has seen critical advancement in the development of modeling formulations that characterize CP individuals' musculoskeletal morphologies and function, a central element driving this position paper focus towards CP[16, 18, 23].

This paper highlights technologies in; (i) Patient-specific segmental rigid body models developed from Magnetic Resonance Imaging (MRI) for use in inverse kinematics and inverse dynamics pipelines; (ii) Efficient population based approaches to derive skeletal models and muscle origins/insertions that are useful for population statistics and consistent creation of continuum models; (iii) Continuum muscle descriptions to derive muscle arc-lengths including spatially varying material properties with muscle wrapping; (iv) Muscle tendon properties specific to CP; and (v) Neural-based and electromyography (EMG) informed musculoskeletal modelling for simulating movement at the interacting neuro-mechanical levels.

2 Multibody clinical gait analysis for children with cerebral palsy

Children with CP are by far the largest patient population who undergo three dimensional (3D) movement analyses. In 2015 more than 60% of children seen by the Queensland Children's Motion Analysis Service were diagnosed with CP. There is no doubt that results from clinical motion analysis are useful in the clinical decision making process for children with CP [24, 25]. However, approximately 23% of patients still experience negative outcomes even when the recommendations from 3D motion analysis are followed[24, 26] potentially due to disparity in choice of surgical procedures performed across clinical facilities for a similar gait profile [27].

Traditional 3D clinical gait analysis methods provide information to estimate joint kinematics and joint kinetics, but do not provide direct objective information to assist with planning of these complex surgical procedures[28]. In recent years, user friendly

musculoskeletal (MSK) modeling software (e.g. OpenSim[29] and AnyBody[30]) has enabled calculation of muscle-tendon lengths[31], moment arms[32], forces [33] and joint contact forces calculations[34, 35]. These data can be used to perform muscle-driven dynamic simulation to understand muscle contributions to joint and center of mass accelerations[36, 37]. In this context, accurate estimates of muscle-tendon force can provide quantitative metrics for clinicians to guide assessment of abnormal motor function and devise targeted treatments in simulation before application to the actual patient.

MSK models are computational representations of a person's MSK anatomy. The models consist of multibody systems including rigid bodies (bones) connected by joints and actuated by muscle actuators producing force according to physiological behavior[29, 38-41]. In these muscle actuators are represented as curvilinear pathways passing through via points or around warping surfaces. The MSK anatomy are generally derived from dissections of adult cadaveric specimens[42-46] and used to implement generic models[38, 39, 41]. In common applications, these models are linearly scaled to fit the anthropometry of individual subjects using information from 3D motion capture and/or anthropometric measurements. However, in the clinical setting it is arguable whether these additional information from MSK models can assist in surgical planning [47] or whether the kinematic, kinetic and muscle tendon results accurately and reliably reflect pathological locomotion [48, 49]. Moreover, the generic nature of the MSK models employed mean they may not account for the muscle contracture, spasticity and bony deformities experienced by the children with CP. The conventional anatomical model used in clinical gait analysis [50, 51] is based on joint center positions and axes estimated from the spatial trajectories of skin-mounted reflective markers and a limited number of anthropometric measurements. Inertial properties of the body segments are estimated using regression equations [52].

2.1 Skeletal models

The anatomical parameters included in generic MSK models are representative of an adult (or elderly) musculoskeletal geometry, generally not pathological (dissections were generally performed on specimens with no reported musculoskeletal diseases) and do not provide an accurate representation of the skeleton in the pediatric population, let alone the deformed pediatric population [53, 54]. This is important because outputs from dynamic simulations are sensitive to the geometry of the skeleton, joints definition and muscle attachments locations [55]. For example, Bosmans et al., [56] generated scaled generic and subject-specific musculoskeletal models to investigate the effect of aberrant proximal femoral bone geometry on hip joint contact forces and showed that scaled generic musculoskeletal models masked the real orientation of the hip joint contact force. Therefore, a first challenge for investigations on CP based on MSK models is the personalization of bone geometries, especially when alterations are evident compared to typically developing anatomy. The typical pediatric population has a large amount of variation in lower limb bone geometry, which continues to change throughout growth[57]. Children with CP commonly develop a progressive internal femoral torsion deformity that reduces the mechanical advantage of muscles that cross the hip joint (i.e. hip abductors and glutei) leading to less efficient muscle contribution to locomotion[50, 58]. Many children with CP also walk with excessive flexion at the hip, knee, and ankle (i.e. crouch gait) and develop an external tibial torsion deformity[10, 59]. With advancement in medical imaging it is now feasible to incorporate accurate measures of femoral and tibial torsion in the clinical pathway[60-62].

Several applications of MSK models to CP are available in the literature, although most have not considered bony geometrical alterations in their models[33, 35], but used linearly scaled generic models[39]. In other studies, the generic model was personalized by including selected features of the patient geometry, such as femoral or tibial torsion[53, 59]. More

comprehensive personalization has also been proposed by fully morphing a generic model, e.g. by Oberhofer et al.[63]. In recent years, the possibility of acquiring medical images, especially MRI, has made available to clinicians and researchers a source of anatomical information *in vivo*. Manual or semiautomatic segmentation of muscles and soft tissues, combined with the use of specialized software such as NMSBuilder [64], allows the generation of patient specific (bone geometry and muscle paths) kinematic and kinetic models that can be used for patient assessment. The increasing complexity that can be captured by MSK models can be seen in Figure 1. Musculotendon actuators, briefly discussed below, can be included in the models as well, although their definition requires a considerable effort in pre-processing and model preparation.

Subject- or patient-specific segmental and skeletal models have recently been developed for clinical gait analyses[65]. Using geometrical representations of the patient's bones, it is possible to identify joint parameters based on their shape. In lower limb models, the hip joint is represented as a ball and socket joint, whose center is located by fitting a sphere to the femoral head [64, 66]. However, this choice may poorly represent a severe hip joint dysplasia and joint deformation resulting in risk of hip dislocation [67]. The knee joint is often modeled as a hinge, by defining the epicondylar axis [68] or by fitting spheres to the condyles[48, 65, 69]. The ankle joint is also modeled as a hinge, with the axis defined by a cylinder fitted to the trochlea surface of the talus[70, 71] or by the line going through the centers of two spheres fitted to the medial and lateral aspects of the trochlea [72]. Both the knee and ankle joints can be implemented using more complex models, which include the constraining effect of the ligaments on the (passive) joint kinematics by considering them as inextensible [73] or minimally extensible [74]. Examples of personalized joint models from medical imaging include the use of MRI [66, 75], low dose biplanar X-ray [76] and freehand 3D ultrasound [77].

It is worth noting that MSK modelling software generally uses inverse kinematics approaches to calculate joint angles from 3D experimental data [78-80], while traditional gait analysis relies on direct kinematics [51]. These two techniques are conceptually different and a thorough comparison is necessary before being able to quantify the differences between generic and patient-specific models[65]. The inclusion of markers visible in the MRI scans and collection of gait analysis data just after the medical images can lead to reduced error in placing virtual markers in the inverse kinematic procedure[65].

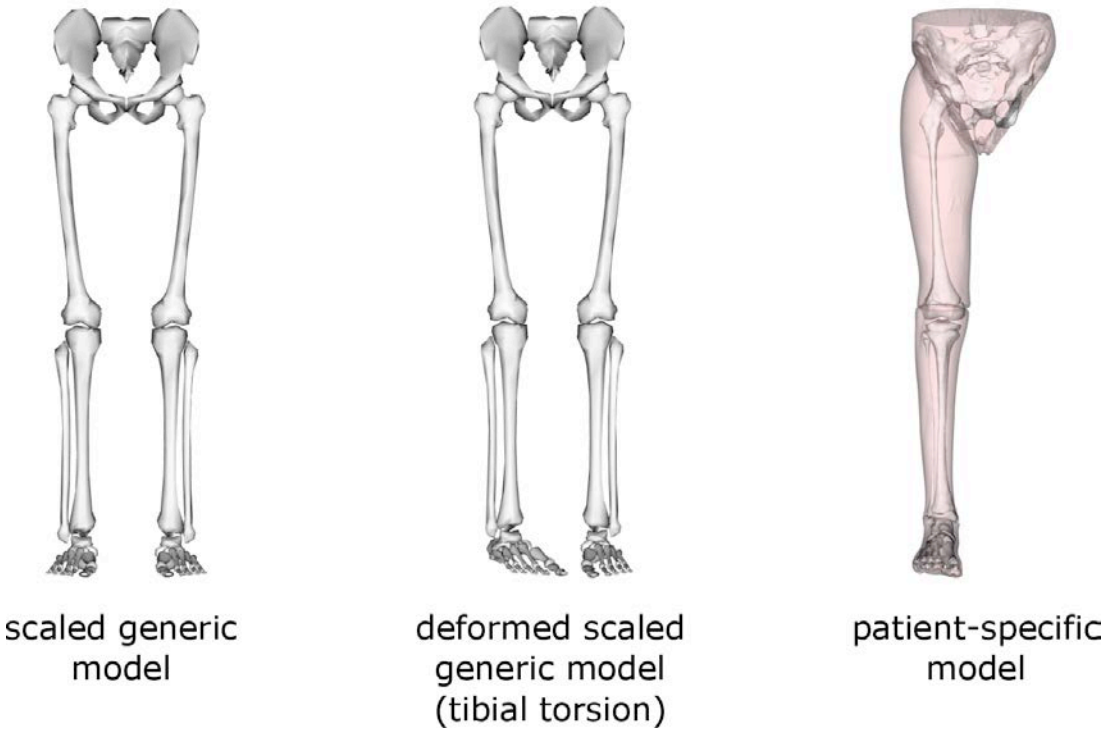

Figure 1 Varying amount of subject-specificity in relation to representing the skeletal system of children with cerebral palsy; a generic scaled model (left), a generic scaled model including some specific deformations, e.g. 30 degrees tibial torsion (centre), and a subject specific model obtained from medical images (right).

From the knowledge of joint kinematics and the external loads (i.e. ground reaction forces), and estimated inertial properties of the body segments[81, 82], net joint moments can be

determined using the inverse dynamics analysis[83]. Using subject specific models derived from MRI (Figure 1, third model) it is possible to calculate subject specific inertial properties, assigning different densities for bone and soft tissues[84, 85]. This is especially valuable when assessing individuals out of the ranges of the data used to generate the regression equations, e.g. obese patients and children with altered anthropometric proportions.

2.2 Case report of subject specific modeling of a child with cerebral palsy

The case report highlighted in Figure 2 suggests that, at least in the sagittal plane, the conventional models from gait analysis and the subject specific models can produce similar evaluation of the joint kinematics, kinetics and powers. In Figure 2, a subject specific model where all joints were modeled as ball and sockets is compared to results obtained using Vicon Plug-in-Gait. In these simulations the traditional and patient-specific models were driven using MRI-visible markers. The agreement between the two methodologies is important in at least two aspects: 1) it means that normal practice standard gait analysis is an appropriate tool for (this) patient assessment, and 2) it suggests that if patient-specific models were introduced in clinical practice, for instance coupled with further analyses such as musculotendon lengths or force estimation, they could add subject-specific information while maintaining consistency with a more traditional evaluation of the patient's neuromuscular function. This would also provide clinicians with biomarkers that direct relate to CP individuals' musculoskeletal function. This would facilitate objective quantification of patients' motor capacity throughout rehabilitation treatments and help control subjective judgment often associated with the use of clinical scales (i.e. Fugl-Meyer)[14].

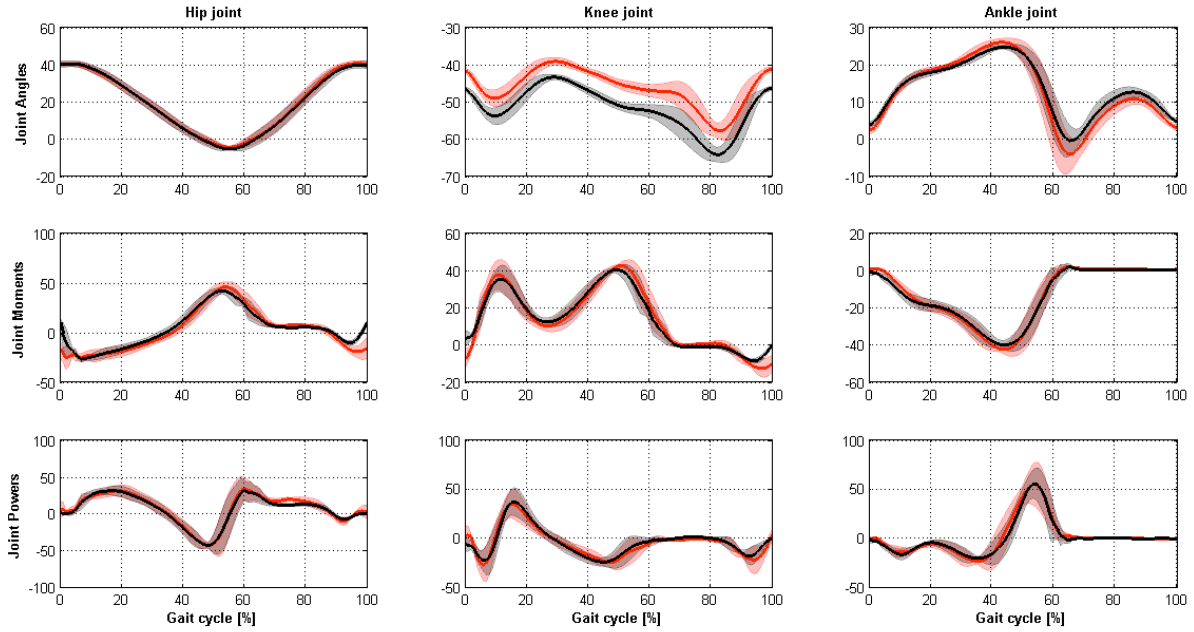

Figure 2 Example of joint angles, joint moments and joint powers obtained using the conventional model (Plug in Gait, in red) and a fully subject specific kinematic and kinetic model (in black). Results are presented only for the sagittal plane.

3 From rigid-body to continuum models using statistical models

Modelling the biomechanical impact of CP at the tissue level requires applying the kinematic and force boundary conditions derived from rigid-body models to continuum models of tissue mechanics and response. Rigid-body models commonly use sparse or coarsely scaled bone and muscle geometry[86, 87], while continuum models, such as finite-element models, require accurate, patient-specific geometry often segmented from 3-D medical images[88]. Segmentation of bones, and muscles, is time consuming, and prone to subjective errors. Statistical models can be used to predict 3-D anatomy from sparse data[89], thereby bridging the disconnect between rigid-body and continuum models and improving the clinical applicability of computational models in CP therapy.

3.1 Bone model generation

Cerebral palsy causes deformities in both the shape[90] and density[91] of bones. These deformities impede normal function, such as walking or reaching tasks, and also lead to higher risks of osteoarthritis (OA), dislocation, and bone fracture[92]. Given the large spectrum of severity in CP deformities[93], continuum models of bone, combined with statistical models of bone morphology variation, can predict the efficacy of therapies in reducing the risks listed above for different variations of CP.

Statistical models of bone shape[94] and bone mineral density (BMD) distribution[95] efficiently capture the variations in 3-D bone morphology across a population. Such models are "trained" on a set of data (the training set) sampled from a population of interest. In the case of a shape model, this typically involves segmenting surfaces, re-parameterizing each surface in a correspondent manner (e.g. a common mesh topology), then registration to remove similarity transforms between the surfaces. A dimensionality reduction method such as principal component analysis can then be applied to the aligned surfaces to reveal significant modes of shape variation and/or clusters or shapes. In the case of a statistical model of BMD distribution, surface parameterization and registration are replaced by image registration. Such models, once trained, can be used to predict full 3-D morphology from sparse data[89], make classifications, and quantify the difference between specimens[96, 97].

We have demonstrated shape model based workflows for generating 3-D morphology from sparse data[98]. These workflows combine data routinely collected in gait laboratories (motion capture marker coordinates, anthropometric measurements) and partial segmented surfaces (e.g. from the hip or knee) to generate 3-D surface meshes of the pelvis, femur, patella, tibia, and fibula. The meshes can be used as rigid-body shells for joint contact simulations[99] to study the development of osteoarthritis in CP, or volumetrically meshed for finite-element or multiscale models of the bone tissue[100]. The use of statistical models in the

model generation process ensures anatomically feasible geometries and clinically feasible runtimes of minutes.

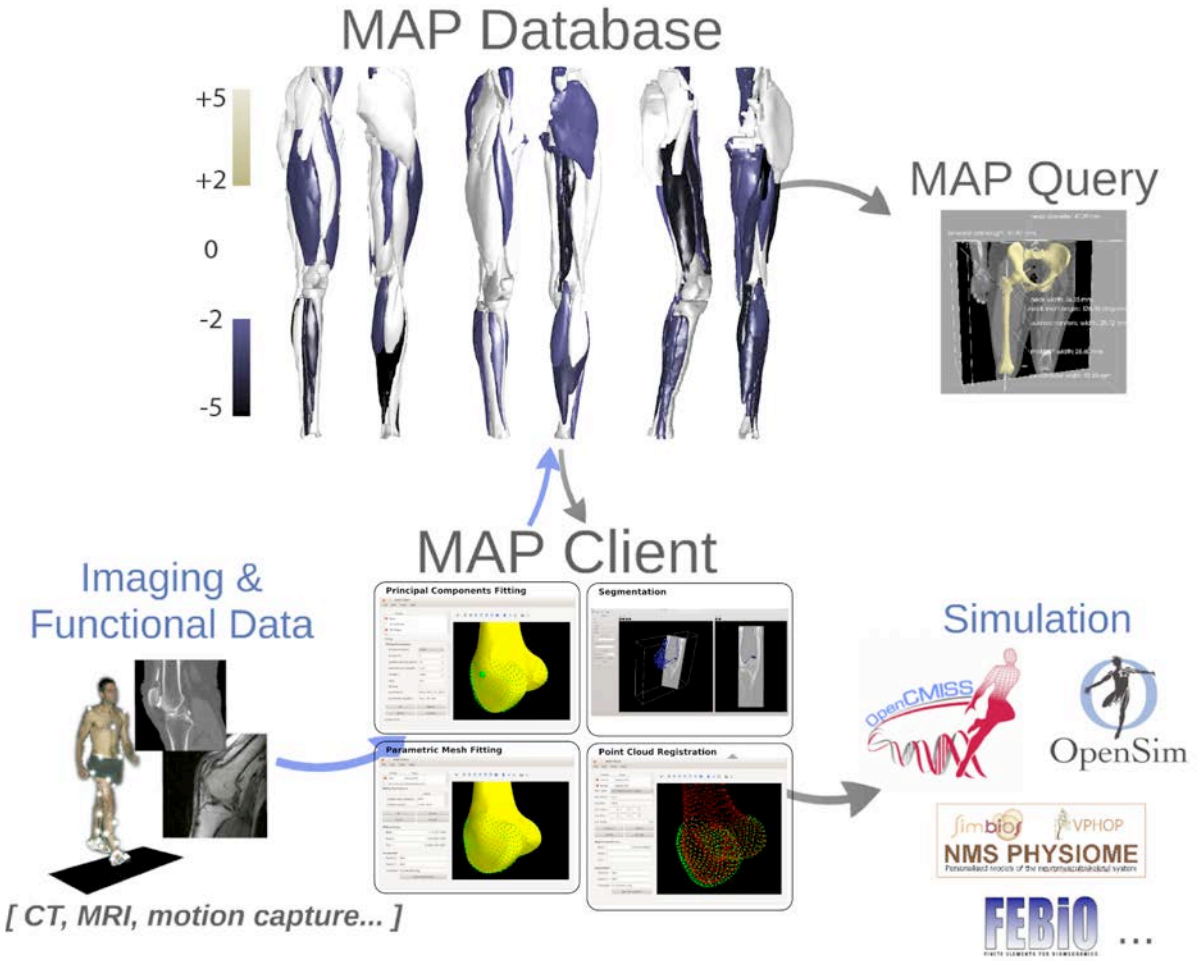

Figure 3: The Musculoskeletal Atlas Project provides workflows for generating musculoskeletal models from clinical data using statistical models. The MAP Client software manages plugins that perform steps such as model registration and mesh fitting. These steps can use data from the MAP Database for typically developed or cerebral palsy populations (CP limbs shown with significantly small muscles highlighted according to Z-score). The generated models bridge the gap between rigid-body and continuum models.

These workflows have been implemented in the open-source Musculoskeletal Atlas Project (MAP) Client software and are freely available to the community[98]. The MAP (Figure 3) aims to consolidate into one common platform the many steps involved in musculoskeletal model generation (e.g. segmentation, registration, and mesh-fitting) as well as the statistical models on which they depend. Going forward, we see the MAP and MAP Client as useful

tools in the CP-oriented musculoskeletal modeling environment, as well as tools that can promote the use of computation modeling in a clinical setting.

3.2 Generative three-dimensional models of muscle

Cerebral palsy is associated with muscle weakness[101], alterations in neural drive[102], and altered mechanical properties of muscles[103]. There may be significant shape variations in CP muscles as well. The use of statistical methods and data driven modeling is promising for processing, classifying, and analyzing 3-D datasets of muscle shape and size for CP. Thorough knowledge of CP-specific muscles will greatly aid CP modeling in rigid body models, but may also contribute to the use of continuum muscle models in rigid body frameworks, thus bridging the gap between these two modeling approaches.

As with bone and joints, subject-specific muscle shapes and sizes are often generated from manual or semi-automatic segmentation of medical images[88, 104-107], which is extremely time-consuming and often relies on subjective judgments by the user. In contrast to segmentation of bones where cortical or trabecular bone can be distinguished from neighboring tissues, muscle segmentation generally requires classifying neighboring and sometimes non-distinct regions of muscle tissue into specific distinct muscles. Statistical shape models of muscle are a promising tool that may improve automated muscle segmentation routines by providing statistically informed targets for muscle shape, size, and location that can constrain computer vision and image processing routines.

Cerebral palsy is a heterogeneous diagnosis[93] and recent research has shown that muscle sizes in children with CP are heterogeneously distributed (Figure 3)[104]. The breadth of manifestations of CP make statistical shape modeling a particular challenge; however, with sufficiently large training datasets and data-driven modeling approaches, muscle size and shape relationships and classifications may be achieved, allowing subsequent predictions

from sparse data. The accurate and fast determination of muscle size and shape information in subjects with CP will benefit rigid body modeling directly by providing more realistic inputs for relative muscle sizes in solving force optimizations[86, 87]. In the future, it will also serve to introduce more sophisticated, continuum-level muscle models into a rigid body framework and enable greater use of models to answer clinical and surgical questions regarding CP[87, 108, 109].

4 Continuum descriptions of muscle

Muscle fiber orientations, moment arms and muscle contact interactions in CP are also likely to vary considerably from the general population. Continuum descriptions of muscles allow for spatially varying fiber orientations, muscle interaction including sliding and wrapping around the skeleton giving improved estimates of muscle moments arms and musculotendon lengths. Integration of continuum based muscles with free form deformation (FFD), a computer graphics morphing technique, can be used to efficiently morph underlying muscle geometries modeled with many degrees of freedom using a coarse enclosing mesh with only a few degrees of freedom. The coarse mesh is morphed so as to minimize the distance between strategically chosen control points (from MRI or motion capture) and this deformation is passed to the embedded muscle structures within. This idea was first demonstrated by Fernandez et al.[110] using generic template muscle meshes developed from the popular Visible Human data set[111]. The FFD method provides shape control over muscle curvature and length by using shape-based constraints called Sobelov smoothing [112]. FFD can be performed at the individual muscle and bone level or be applied to the outer skin and whole muscle groups. Figure 4 shows FFD being used where the host is the skin with embedded muscles being internally deformed based on skin motion. Control points can be

located on the skin surface or within the limb and be used to control internal muscle deformation.

Muscle fiber information is a key component of muscle function, as it controls the direction of muscle contractile behavior and shape in 3D, and the pennation components of force in 1D Hill-type models. In 3D finite element muscle models, extracted fiber information from both cadaver dissections and MRI has been used to inform spatially varying fiber architecture[113-115]. Figure 4 shows a representative dissected cadaveric human rectus femoris muscle with visible fiber pennation angle. Discrete fiber angle measurements were made at different slices and mapped to a continuum fibre field, which becomes part of the generic muscle template.

In gait analysis, continuum muscles have been used to inform rigid body mechanics simulations with anatomically correct musculotendon arc-length paths and muscle moment arms. FFD requires high numbers of control markers, which is difficult to achieve in practice. This limitation has been partially addressed by introducing additional non-kinematic information including material behavior (constitutive laws), tissue interaction (contact mechanics) and volume conservation constraints[116]. Muscle arc-length centroids can be used to perform a virtual tendon excursion and evaluate moment arms. Figure 5 shows a hybrid finite element-FFD approach with wrapping surfaces, muscle sliding and bone interactions for the semimembranosus and semitendinosus muscles through 45° hip flexion. This extension to traditional FFD couples FE analysis allowing different material laws to be included accounting for stiffer tendon, spatially varying fiber fields, soft tissue sliding and volume conservation of muscle generating a more anatomically realistic shape with only a few control points needed.

This technique was further evaluated for the complete lower limb by Oberhofer et al. [63] by matching MR segmented geometries at 15° and 45° flexion with host-mesh predicted muscle shapes producing errors less than 3.7 mm RMS (Figure 5 lower). The FFD morphing method provides complex muscle scaling to patient data beyond the simple scaling currently offered in OpenSIM. The predicted deformations of five muscles were validated using MRI data of the same subject in two different lower limb positions. The walking model was considered the first of its kind, allowing the realistic deformation of several muscles throughout gait with reasonable computational costs.

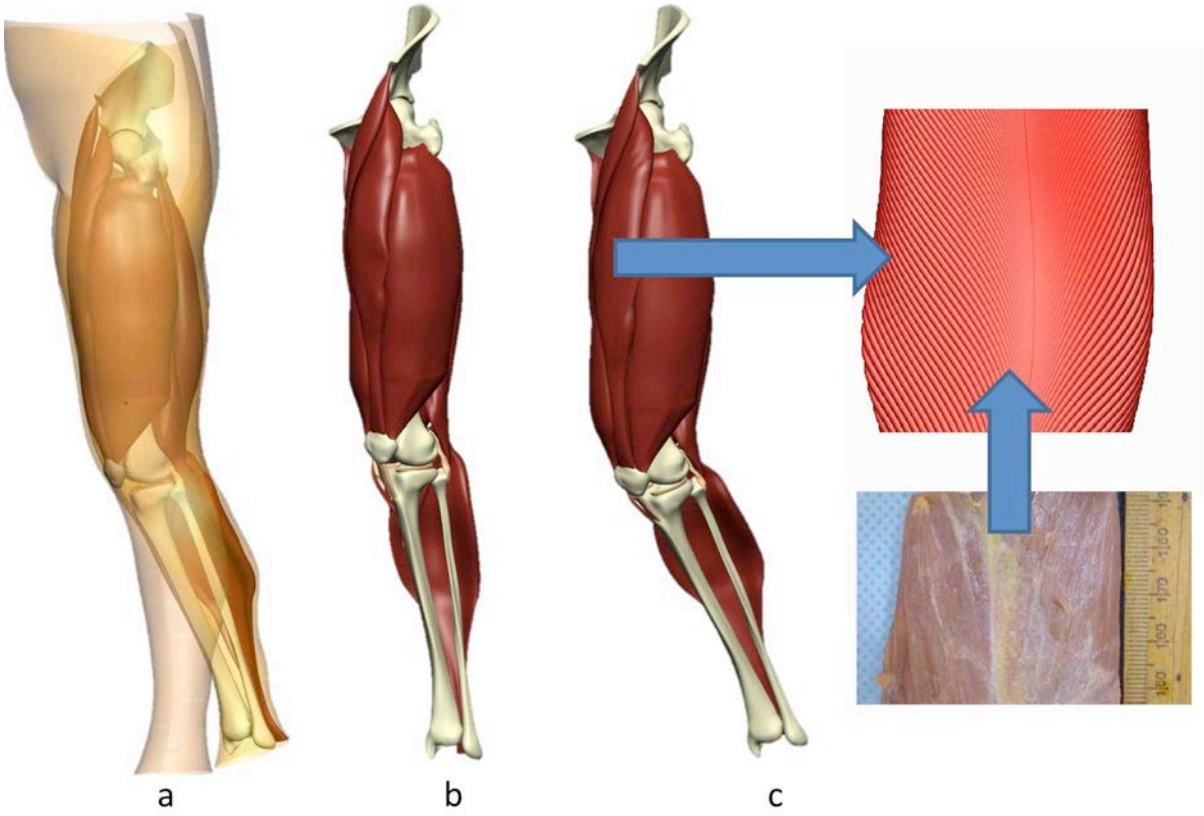

Figure 4: (a) Complete lower limb skin host-mesh with embedded muscles deformed using motion capture surface markers. (b) Initial embedded muscle pose and (c) resulting deformed muscle pose after 30 degrees flexion. Highlighted is the bipennate fiber field fitted for the rectus femoris muscle derived from cadaveric images.

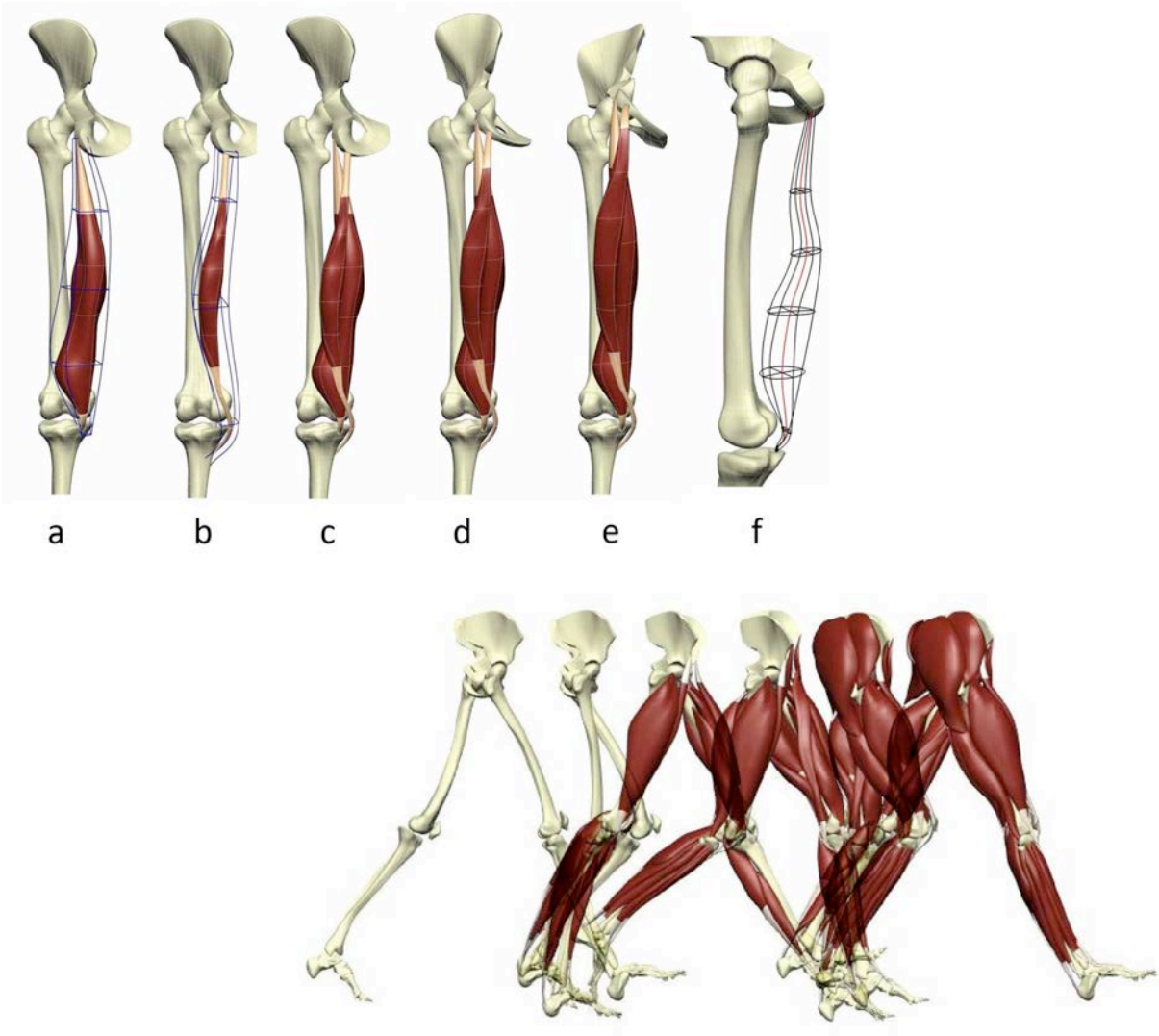

Figure 5: Top (a) Semimembranosus and (b) semitendinosus muscles embedded inside hybrid mechanics host volume meshes. (c-e) Finite elastic mechanics simulations of muscle deformation, sliding and wrapping through 45 degrees of hip flexion; and (f) muscle arc-length changes through muscle centroid (red). **Bottom** Soft-tissue muscle deformation during walking was derived from the deformation of a surrounding skin mesh based on inverse kinematics, i.e. segmental kinematics. The predicted deformations of five muscles were validated using MRI data of the same subject in two different lower limb positions.

5 Muscle adaptations in children with cerebral palsy

Whether using rigid multi-body or continuum model representations of muscle, muscular architecture is the primary determinant of muscle function[117] and the specific musculotendinous adaptations in CP contribute to a loss of muscle strength[7] and functional ability[118]. Individuals with spastic-type CP have reduced muscle volume, increased intramuscular fat, reduced or similar muscle fascicle lengths, increased muscle fascicle stiffness, and increased Achilles tendon length compared to their typically developing peers[119-123].

A review of gross muscle morphology and structure in the lower limb of children with spastic-type CP found consistent evidence for reduced muscle size with muscle volume reduced in the most impaired limb compared to the less impaired limb and muscles of children with typical development.[101] The majority of studies investigating muscle volume focus on the calf (triceps surae) muscle. The calf is commonly impaired in children with spastic-type CP and it is frequently the target muscle for intramuscular Botulinum toxin type-A (BoNT-A) injections to reduce spasticity and correct equinus gait in addition to surgical and conservative treatments[124, 125]. It is an important muscle because it provides vertical support and forward propulsion during walking.[126] In ambulant children with spastic-type CP the volume of the impaired calf muscle is reduced by 22-57%[121, 123, 124, 127, 128] compared to children with typical development with differences in calf muscle volume already present by the age of 2-5 years,[119] (Figure 6A). The decline in force-generating capacity of the muscle throughout the range of motion of the ankle has been directly attributed to reduced muscle volume,[120] (Figure 6B). In addition, a higher intramuscular fat content translates to a reduced proportion of contractile tissue within the muscle, which also contributes to weakness.[122]

Increased passive joint stiffness (non-neurally mediated) in subjects with upper motor neuron lesions has been attributed to shorter muscles and muscles with shorter fascicles,[129,

[130] (Figure 6C). However, conflicting findings of studies comparing fascicle length on the paretic side in individuals with spastic-type CP and in typically developing individuals have been reported, with some studies reporting reductions in fascicle length,[131, 132] while others report no differences.[133, 134] These studies of in vivo muscle architectural properties in spastic-type CP have primarily been confined to measurements of resting fascicle length/angle. These measurements are typically made at the resting joint angle, where muscle tension is assumed to be negligible, and so do not reveal information about muscle stiffness. In the only study to date investigating passive mechanical properties at the fascicle level, the medial gastrocnemius fascicle has a shorter slack length (fascicle length when torque exceeded 0 Nm of plantar flexor torque) and undergoes 47% less strain in spastic-type CP compared to controls at approximately equivalent passive ankle torques, suggesting that muscle fascicles have a greater resistance to passive stretch in spastic-type CP,[119] (Figure 6B).

The Achilles tendon interacts with the triceps surae muscles and plays an important role in force transmission and energy storage and return during functional activities. Importantly, the length and compliance of the Achilles tendon can uncouple the length changes of the fascicles from that of the muscle–tendon unit, and thereby influence the force-generating capacity of the muscle[135]. Examination of the gross tendon structure and function in individuals with spastic-type CP reveal that the Achilles tendon is longer, thinner, and contributes more to passive muscle-tendon lengthening, compared to typically developed peers[136-140].

Alterations to the musculotendinous unit and neural control have direct implications for functional performance in ambulant individuals with spastic type CP. Altered muscle-tendon unit function during walking[141, 142] contribute to reduced power generation during gait[143], which in turn diminishes anaerobic performance[144] in children with CP. Strength is

moderately associated with walking speed[145] and activity limitations[5] suggesting that muscle adaptations in children with spastic-type CP plays a key role in difficulties with functional mobility in children with CP.

From a clinical perspective, the ability to estimate pre-treatment levels of muscle stiffness or contracture in an individual patient would enable quantifying the major muscular determinants underlying CP motor function. This would be precious information for predicting changes in muscle function following interventions such as intramuscular Botulinum toxin injections and surgery.

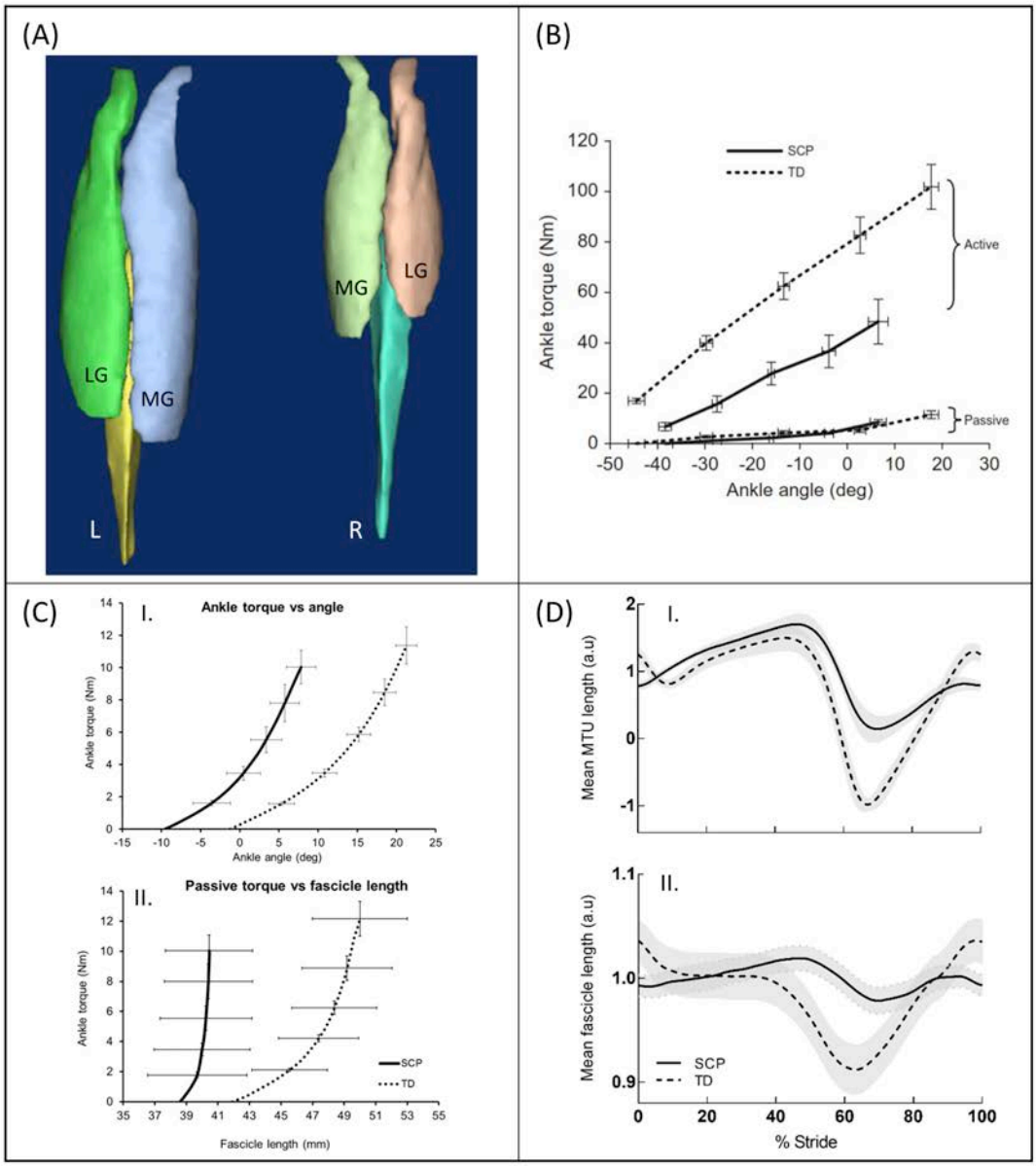

Figure 6. (A) MRI scan of both lower legs (L=left, R=right) of a child with spastic type cerebral palsy (SCP, right hemiplegia). Medial (MG) and lateral (LG) gastrocnemius muscles are segmented to measure muscle volume; (B) Active muscle properties, ankle torque versus angle, of individuals with SCP and typically developing (TD) peers (mean±SEM); (C) Passive muscle properties [I] ankle torque versus angle, [II] ankle torque versus MG fascicle length of individuals with SCP and TD peers (mean±SEM); (D) LG Muscle-tendon unit and fascicle functional during one stride of walking gait in individuals with CP and TD peers, 0% stride = initial foot contact

6B Reprinted from Journal of Biomechanics, 45(15): 2526-2530, Barber, L., Barrett, R., Lichtwark, G., Medial gastrocnemius muscle fascicle active torque-length and Achilles tendon properties in young adults with spastic cerebral palsy. Copyright (2012), with permission from Elsevier.
6C preprinted from Journal of Biomechanics, 44(3): 2496-2500, Barber, L., Barrett, R., Lichtwark, G., Passive mechanical properties of the medial gastrocnemius muscle in young adults with cerebral palsy. Copyright (2011), with permission from Elsevier.

6 Neural-based modeling control of locomotion

CP underlies disrupted function in the central nervous system. This needs to be first characterized and then incorporated in patient-specific MSK models to enable examining cause-effect relations with the resulting disrupted function at the musculoskeletal level.

Advances in neurophysiology are helping characterize the neural processing underlying human movement, i.e. the generation of synaptic inputs ultimately converging to pool of motor neurons and the transmission of the resulting neural drive to the innervated muscle fibers (Figure 7). The combination of a motor neuron and its innervated muscle fibers form a functional unit, called “the motor unit”, which operates for transducing neural inputs to mechanical muscle force[146, 147]. Advances in electrophysiology are contributing to address the long-standing question of how the central nervous system handles the large number of movement degrees of freedom (DOFs). Increasing experimental evidence is demonstrating how specific motor unit action potentials are not the result of dedicated synaptic inputs sent to individual motor neurons, but the result of a common drive to a motor neuron pool to which individual innervated muscle fibers respond differently because of specific intrinsic properties[146]. The concept of muscle synergies extrapolates to the macro-scale by supporting the existence of coordinative neural macrostructures, explicitly encoded in the central nervous system, that reduce the computational burden in the neural control of many fibers, from many muscles, during complex motor tasks[148] (Figure 7). Despite these advances, electro- and neuro-physiological analyses alone cannot explain the mechanical significance of the experimentally observed neuromuscular mechanisms[149].

Advances in gait analysis and MSK modeling are enabling understanding movement mechanics at the level of the underlying muscle forces, something central for investigating

how people solve for motor control in locomotion (Figure 7)[150]. Current methods largely rely on optimization where muscles are recruited according to pre-defined criteria such as minimizing the sum of squared muscle activations, so that the emerging muscle-actuated movement tracks reference joint mechanics[151], or shows agreement with joint mechanics normative values[152], with additional control objectives such as minimal metabolic cost of transport[153]. However, it is not possible to know *a priori* what the nervous system really optimizes. Therefore, the choice of one optimization criterion may substantially impact the computation of muscular and articular forces, thus biasing the final musculoskeletal analysis[154, 155]. These approaches generate systematic and repeatable muscle force patterns that may be valid in specific conditions, but may not encompass an individual's neural repertoire, i.e. inability of synthetizing how neuromuscular patterns vary across subject-specific, context-dependent conditions including time, training, fatigue, pathology, motor tasks.

An alternative is that of building neural data-driven modeling formulations, i.e. formulations that use muscle electrophysiological recordings, rather than optimization, to solve for the muscle recruitment and force distribution problems (Figure 7)[40, 147]. The idea is to use muscle electrophysiological recordings, such as electromyograms (EMG), in conjunction with advanced processing techniques to gain experimental access to neural information underlying an individual's motor function and pathology (Figure 8A). This enables deriving experimental estimates of subject-specific, context-dependent, and realistic neuromuscular strategies with no need to make *a-priori* assumptions on neuromuscular recruitment. This is especially valuable for estimating of pathology-dependent neuromuscular strategies with no need for creating complex numerical models of pathological neuromuscular function, which would be difficult to validate and therefore translate to the clinical level. Direct or indirect estimates of the neural drive to muscles will be termed as

"neural excitation".

Following this rationale we have extracted neuromuscular features from surface EMG data including motor unit firing events[19, 147] (Figure 8A), linear envelopes (Figure 9)[147, 156] and muscle synergies (Figure 8B)[157]. Linearly filtered envelopes enable demodulating the raw EMG and recover amplitude information proportionally to the neural drive received by individual muscles. However, the recovered amplitude may not necessarily be a direct reflection of motor unit spatial and temporal firing due to limitations that include electrode placement, detection volume, and motor unit action potential superposition[146]. High-density EMG in conjunction with blind-source separation is now an established approach for discerning the interference EMG signal into the constituent motor unit activity and for resolving the inherent problem of motor unit action potential superposition (Figure 8A)[147]. Synergies reflect low-dimensional, linear approximations of EMG statistical structure and distribution. They are derived using unsupervised machine learning methods such as non-negative matrix factorization[158] and enable capturing the elementary modules of multi-muscle co-excitation that are descriptive of a specific regime or motor condition, i.e. locomotion (Figure 8B).

EMG has been successfully used to derive excitations as a direct input to open-loop musculoskeletal models (Figure 7). These are predictive formulations where excitations directly drive muscle fibers and series elastic tendons, i.e. muscle-tendon units (MTUs). The forces produced by the EMG-driven MTUs are used to compute the resulting joint mechanical function blindly, i.e. with no tracking mechanism that accounts for prediction errors (Figure 7)[40, 147, 156, 159]. This paradigm was applied to show for the first time that it is possible to achieve simultaneous, proportional, and accurate estimation of joint moments about six degrees of freedom in the human lower extremity as a direct function of EMG linear envelopes[147]. The theory of muscle synergies was then used to investigate to what

extent muscles are controlled individually or as part of a synergistic scheme, something central for understanding locomotion neural control. It was found that the excitations of 16 lower limb muscles recorded during four biomechanically different locomotion tasks could be well described by a shared lower-dimensional set of five excitation primitives (Figure 8B). Results showed, for the first time, that the five-dimensional primitive set not only reconstructed the experimental EMG data observed across all four motor tasks but also could be used to drive a large scale musculoskeletal model and reconstruct the resulting joint moments generated in six lower extremity DOFs with the same accuracy than when using 16 muscle EMG recordings. This provided further evidence that movement mechanical forces can be generated by neuromuscular strategies operating on a small number of excitation primitives[157, 160]. More recently a robust basis of muscle primitives was derived and showed how this could be used to build predictive models of physiologically accurate muscle excitations across a large repertoire of unseen locomotion conditions[161].

The open-loop formulation was then generalized into a closed-loop modeling formulation that accounts for excitation uncertainties that may contribute to bias the model-based joint dynamics estimates (Figure 9)[154]. These include cross-talk, filtering artifacts and the inability of accessing deeply located muscles. For this purpose, the calibrated open-loop EMG-driven modeling formulation is coupled with a static optimization procedure. This allows extracting muscle excitations by balancing information from experimental EMG data and static optimization solutions. It was shown that a minimal adjustment of experimental EMG data (i.e. root mean squared error, RMSE < 5%), in conjunction with the static optimization solution for the hip flexing iliopsoas MTU, was sufficient to precisely track experimental multi-DOF joint moments during walking and running, with substantial improvement with respect to open-loop formulations[154].

6.1 Investigating movement neuro-mechanical interplay

The closed-loop formulation enabled the computation of muscle force solutions that reflect movement neural and mechanical levels precisely and simultaneously, i.e. muscle forces computed as a function of an individual's minimally adjusted EMGs, which concurrently satisfy experimental joint moments across all lower extremity DOFs (Figure 9)[154]. This paradigm provides the basis to investigate the neuro-mechanical interplay in human locomotion, i.e. understanding the mechanical forces elicited by neuromuscular structures[149].

This opens up to the possibility of predicting a range of mechanical variables that are tightly dependent on neuromuscular mechanisms, difficult to synthetize, such as multi-muscle co-excitation[162]. Important co-excitation dependent mechanical variables include joint stiffness and joint contact force (Figure 7). Pure optimization-based methods alone can only reproduce some of the muscle co-excitation trends within selected locomotion conditions[154], thus limiting the subsequent ability of describing joint contact forces[163] and stiffness[164].

As a result, EMG-informed methods have consistently provided the best predictions of knee joint contact force across the majority of the Grand Knee Challenges past six editions[165, 166], the current gold standard for testing muscle force prediction methods. The They recently, enabled characterizing the dynamics of complex joints such as the hip for which the major flexors (i.e. iliopsoas MTU) are deeply located and inaccessible via surface EMG with predictions validated at the level of *ex vivo* hip joint compressive loads[167]. Importantly, EMG-informed modeling has just now enabled the derivation of dynamically consistent estimates of ankle and knee joint stiffness directly from the joint constituent muscle-tendon units as controlled by EMG-excitations[164].

6.2 Investigating disease processes

The proposed EMG-informed modeling approaches are especially advantageous when investigating neurological conditions like CP, where disrupted and altered neuromuscular function cannot be viably understood and synthetized into computational models. In this context, surface (or intramuscular) EMG has the advantage of providing a clinically viable solution for interfacing with the patient's nervous system *in vivo* and accessing neural information reflecting the specific neurological condition, as exemplified in Figure 8A. This is especially valuable for clinical interventions of limited duration, such as robot-aided rehabilitation[19], where implanted nerve or cortical electrodes would be inapplicable[168, 169].

The ability of mixing excitations from EMGs and static optimization can account for patient-specific neuromuscular strategies and how they vary with time (Figure 9)[154]. Current methods would have limited capacity in capturing non-physiological muscular behavior by means of an arbitrary objective function or basis of muscle synergies. Experimental EMGs could be recorded for target muscles that reflect the patient's non-physiological muscular behavior. These could be used to generate EMG-informed simulations that track patient-specific muscle recruitment strategies and joint dynamics, with patient-specific EMG-to-force relationships.

The ability to translate an individual's EMG activity into joint contact forces and stiffness is central to understand the neuro-mechanics of individuals affected by CP, where muscle contractures and crouched gait would result in both abnormal joint stiffness and contact forces[170]. The ability of understanding cause-effect relationships between altered neuromuscular function (Figure 8A) and altered mechanical function (Figure 9) is central for delivering personalized rehabilitation treatments that restore physiological properties.

In this context, realistic, patient-specific estimates of co-activation dependent variables such as net joint stiffness and compressive loads are important biomarkers for quantifying CP neuro-mechanical determinants, in addition to those discussed in Sections 2 and 5. This would enable direct tracking of joint stiffness and joint loads discrepancies with respect to normative values observed from healthy individuals and would provide a reference for planning treatments such as muscle-tendon lengthening, tendon transfers or osteotomies.

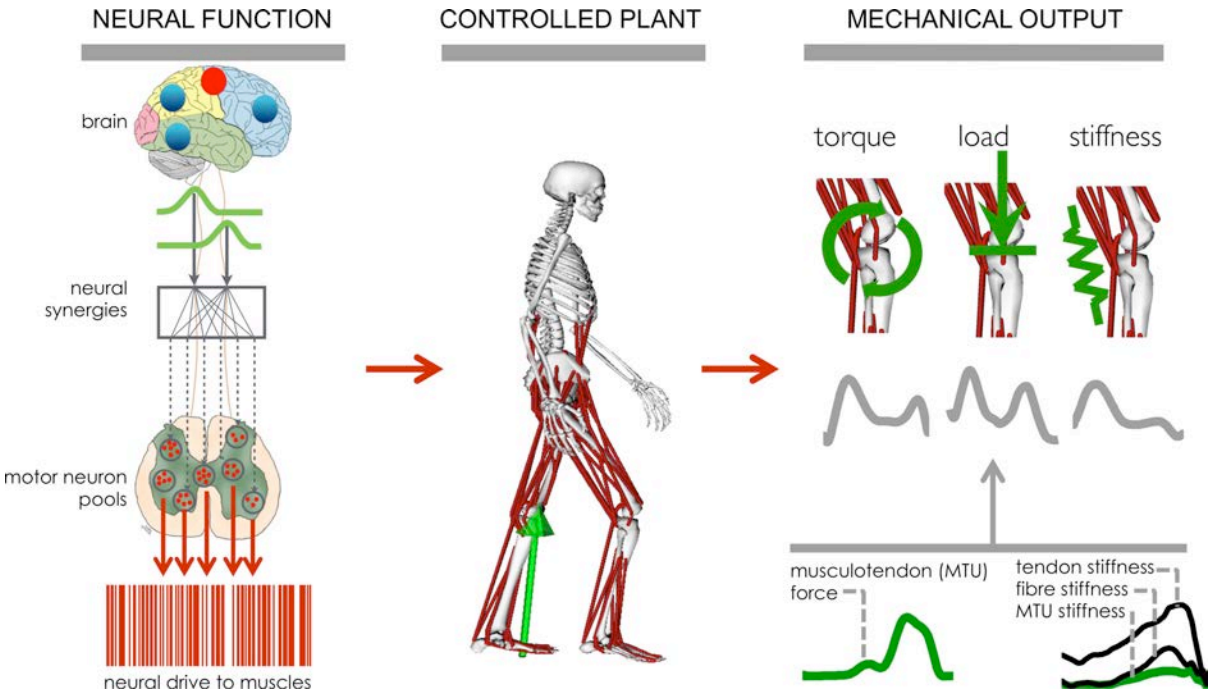

Figure 7: In the execution of a motor task, synaptic inputs are produced as a result of neural microstructures (i.e. neurons) as well as macrostructures reflecting the coordinated interaction between populations of motor, sensory and inter-neurons in the generation of rhythmic motor programs in the spinal cord (i.e. neural synergies). Synaptic inputs ultimately converge to pools of motor neurons, which integrate neural information and transform it into output spike trains (i.e. neural drive) sent to innervated muscles. Neurally controlled muscle-tendon units translate the neural drive into mechanical visco-elastic forces, thus causing articular and segmental body accelerations, multi-joint coordination and compliant body interaction with the environment.

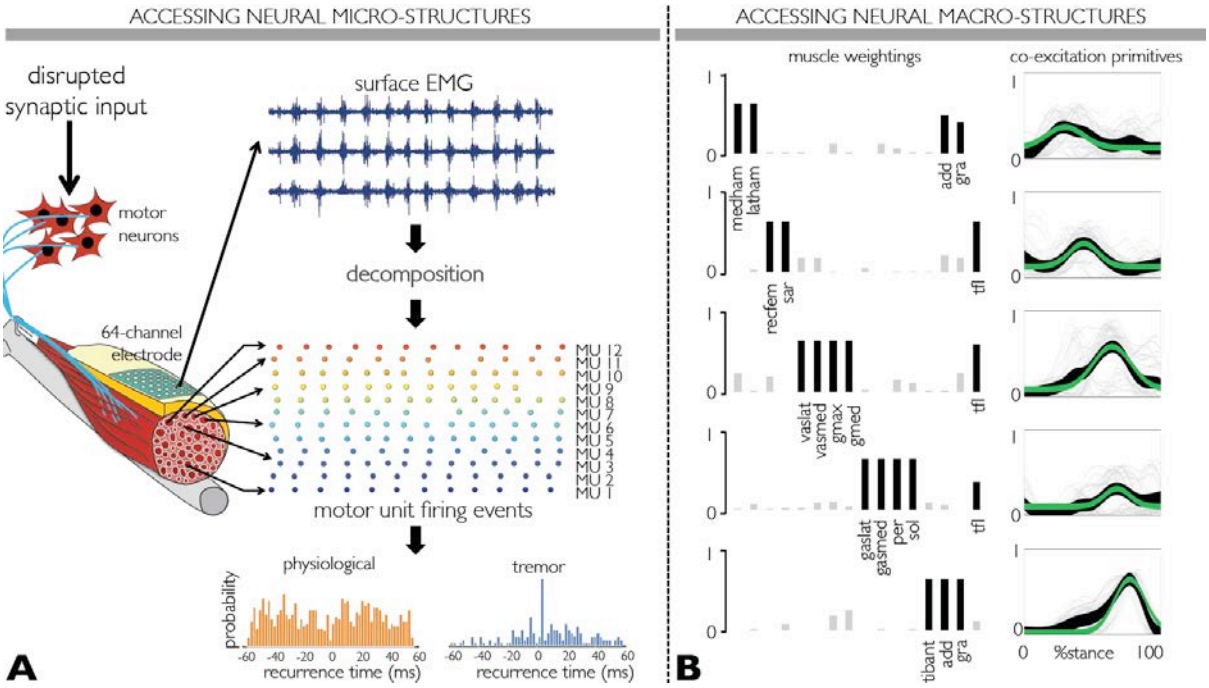

Figure 8: (A) High-density electromyograms (EMGs) are recorded from a tremor patient extensor carpi radialis during a resting task. EMG decomposition discerns the underlying motor unit firings, which corresponds to those produced by spinal motor neurons. In the tremor condition, motor units fire with an abnormally high level of synchronization i.e., see right-hand histogram depicting high probability for any two given motor units of firing within negligible time delays. (B) Five-dimensional synergy structure extracted from 16 lower limb muscles EMGs across four different locomotion tasks. The rhythmicity of the extracted primitives may reflect the dynamics of spinal pattern generators active during cyclic tasks. (A and B) Advanced recording and processing techniques give access to the function of neural microstructures (i.e. motor neurons) and macrostructures (i.e. muscle synergies) *in vivo* in the intact moving human.

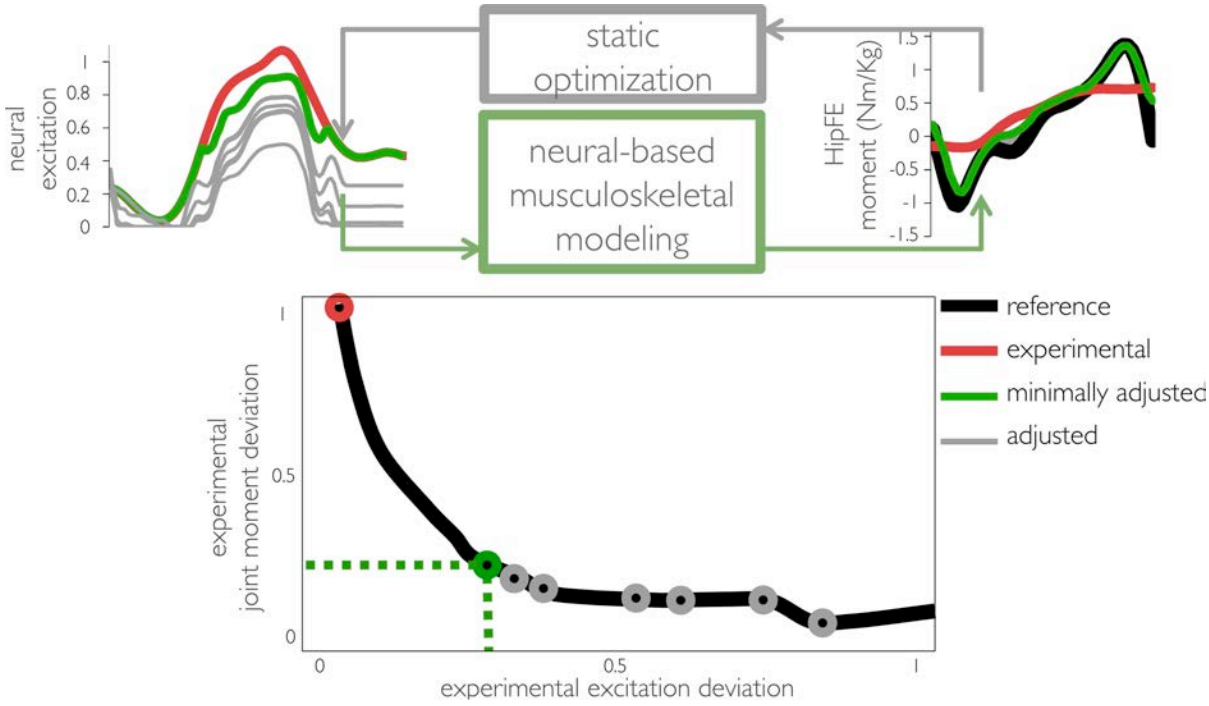

Figure 9: Closed-loop neural-based musculoskeletal modeling formulation. It comprises of two main components: the neural-based forward dynamics musculoskeletal model, and the static optimization component. Recording and modeling uncertainties typically limit forward dynamics prediction capacity. The static optimization component modulates the input excitations to account for forward dynamics prediction errors, i.e. see example gluteus maximus excitation and hip flexion-extension moment prediction error in this figure. In a subject-specific musculoskeletal model, the transfer function between the level of excitation adjustment and moment prediction error is L-shaped, i.e. all dynamically consistent neural solutions exist in a neighborhood of the experimental input data.

7 Challenges and future perspective

A current limitation of patient-specific models is that there is no standard methodology to produce muscle geometries. Mapping techniques from pre-existing atlases [64] and free form deformation methodologies[63, 171] have been presented, but the lengthy processing times required currently makes them far from being clinically applicable. Definition of the muscles is also problematic with respect to musculotendon parameters, which are known to be altered for these clinical populations[120, 172] and play a crucial role in the muscle force generating capacity. Methods relying both on anthropometric dimensions[173, 174] and functional trials[40, 175, 176] have been proposed to estimate the musculotendon parameters required to personalize

generic muscle models [177], but currently none has been used and validated in applications with a CP clinical population.

First the bottlenecks of obtaining anatomical MSK structure from medical images and defining muscles' path and contraction parameters need to be solved. Once done, it will be possible to routinely apply consistent neuromusculoskeletal and finite element models, built from the same patient-specific bone and muscle geometries, to assess MSK tissue loading conditions calculated by the multi-body simulations and applied to equivalent continuous bone models [167, 178]. Biofidelic muscle lines of action [179], joint reaction forces [35, 180] and external forces (inertia and gravity) will be included in the FE simulations, allowing one to investigate tissue loading over multiple tasks and loading conditions previously simulated using musculoskeletal models [178, 181, 182].

While many statistical models have characterized the bones and muscles of healthy populations, building the initial training set is a major challenge for CP populations. Statistical models trained on healthy populations cannot adequately approximate CP-deformed anatomies for accurate model generation. The paucity of data is partly due to the typically young age of patients, which restricts the use of ionizing X-ray CT imaging, particularly around the hip joint; and patient discomfort that restricts time-consuming magnetic resonance imaging. Nevertheless, the collection of large datasets of CP musculoskeletal geometry is essential, and possible through data-sharing initiatives such as the MAP.

Beyond driving the model creation process, a major potential for statistical models is in the classification of CP. Dimension reduction on combined data of bone shape, muscle shape, muscle activation patterns, and functional metrics may identify clusters of CP phenotypes. Computational modelling can determine the optimal therapy for each cluster. A new patient can then be classified based on the cluster they fall within and treated

accordingly. An interesting question will be how well these clusters match current CP classification and treatment strategies. Given the number of anatomical and functional measurements possible and the great degree of variation, data-driven methods offer the best chance to make the best use of clinical data for diagnosis and treatment planning.

The presented MSK modeling methods, based on imaging techniques, population based approaches and continuum muscle descriptions, have the potential of providing high-fidelity patient-specific formulations describing pathological features of muscles and bone structures accurately. However, the associated large computational requirements and challenges in validating resulting predictions may represent additional factors limiting the effective translation to clinical setting. In this scenario, high-fidelity formulations could be synthetized into simpler, surrogate models that describe the complex musculoskeletal structures using computationally efficient structures such as multidimensional splines[159], regressive polynomials[183] or artificial neural networks[184]. These could be coupled with neural based and EMG informed modeling and create fully personalized, clinically viable formulations, which capture neurophysiological, anatomical and morphological abnormalities altogether.

The development of patient-specific neuromusculoskeletal modeling pipelines is central for understanding how neurally controlled muscles elicit joint mechanical function (i.e. rotational, contact and visco-elastic forces) at any particular instant in time. This would fill the gap between current formulations modeling either the neural or the mechanical processes underlying pathological movement[16, 17, 19] and would provide new means for explaining movement function, pathology and recovery. The translation of neuro-musculo-skeletal modeling pipelines to the clinical level is a promising avenue for deriving a new class of biomarkers that directly correlate to a patient's impairment and subsequent recovery. This would complement current assessment techniques based on clinical scales (i.e. Fugl-

Meyer), which often rely on subjective judgment[14] and on indirect estimates of neuromuscular function. Although EMG-informed modeling enables simulations reflecting both movement neural and mechanical levels, the thorough validation of complex pipelines such as the one introduced in this paper is a major challenge for wider adoption and impact in the health care sector. The challenge is to assure that modeling advancements are followed by direct experimental observations of the simulated mechanisms[170]. With complex models being capable of predicting a wide range of musculoskeletal variable there is the need for increasingly more sophisticated experimental techniques for measuring validation data.

The integration of neuromusculoskeletal modeling pipelines in future rehabilitation processes will help objectively reveal how neurological patients can (re)learn and execute large repertoires of motor tasks with direct implications in the development of personalized neurorehabilitation treatments and technologies.

References:

1. Bax M, Goldstein M, Rosenbaum P, Leviton A, Paneth N, Dan B, Jacobsson B, Damiano D. Proposed definition and classification of cerebral palsy, April 2005. *Developmental Medicine and Child Neurology* 2005, 47:571-576.
2. Sheean G. The pathophysiology of spasticity. *European Journal of Neurology* 2002, 9:3-9.
3. Lance JW. Symposium Synopsis. In: Feldman RG, Young RR, Koella WP, eds. *Spasticity: Disordered Motor Control*. Chicago: Year Book Medical Publishers; 1980, 485-494.
4. Crenna P. Spasticity and 'spastic' gait in children with cerebral palsy. *Neuroscience and Biobehavioral Reviews* 1998, 22:571-578.
5. Damiano DL, Quinlivan J, Owen BF, Shaffrey M, Abel MF. Spasticity versus strength in cerebral palsy: relationships among involuntary resistance, voluntary torque, and motor function. *European Journal of Neurology* 2001, 8:40-49.
6. Bache CE, Selber P, Graham HK. The management of spastic diplegia. *Current Orthopaedics* 2003, 17:88-104.
7. Nooijen C, Slaman J, van der Slot W, Stam H, Roebroeck M, van den Berg-Emons R, Learn2Move Research G. Health-related physical fitness of ambulatory adolescents and young adults with spastic cerebral palsy. *J Rehabil Med* 2014, 46:642-647.
8. Hanna SE, Rosenbaum PL, Bartlett DJ, Palisano RJ, Walter SD, Avery L, Russell DJ. Stability and decline in gross motor function among children and youth with cerebral palsy aged 2 to 21 years. *Developmental Medicine and Child Neurology* 2009, 51:295-302.
9. Johnson DC, Damiano DL, Abel MF. The evolution of gait in childhood and adolescent cerebral palsy. *J Pediatr Orthop* 1997, 17:392-396.
10. Kerr Graham H, Selber P. Musculoskeletal aspects of cerebral palsy. *J Bone Joint Surg Br* 2003, 85:157-166.

11. Rodda J, Graham HK. Classification of gait patterns in spastic hemiplegia and spastic diplegia: a basis for a management algorithm. *Eur J Neurol* 2001, 8 Suppl 5:98-108.
12. Stott NS, Piedrahita L. Effects of surgical adductor releases for hip subluxation in cerebral palsy: an AACPDM evidence report. *Dev Med Child Neurol* 2004, 46:628-645.
13. Scholtes VA, Becher JG, Beelen A, Lankhorst GJ. Clinical assessment of spasticity in children with cerebral palsy: a critical review of available instruments. *Dev Med Child Neurol* 2006, 48:64-73.
14. Fasoli S, Fragala-Pinkham M, Haley S. Fugl-Meyer Assessment: Reliability for Children with Hemiplegia. *Archives of Physical Medicine and Rehabilitation* 2009, 90:e4-e5.
15. Lieber RL, Steinman S, Barash IA, Chambers H. Structural and functional changes in spastic skeletal muscle. *Muscle Nerve* 2004, 29:615-627.
16. Steele KM, Rozumalski A, Schwartz MH. Muscle synergies and complexity of neuromuscular control during gait in cerebral palsy. *Dev Med Child Neurol* 2015, 57:1176-1182.
17. Ting LH, Chiel HJ, Trumbower RD, Allen JL, McKay JL, Hackney ME, Kesar TM. Neuromechanical principles underlying movement modularity and their implications for rehabilitation. *Neuron* 2015, 86:38-54.
18. Wang TM, Huang HP, Li JD, Hong SW, Lo WC, Lu TW. Leg and Joint Stiffness in Children with Spastic Diplegic Cerebral Palsy during Level Walking. *PLoS One* 2015, 10:e0143967.
19. Sartori M, Llyod DG, Farina D. Neural Data-driven Musculoskeletal Modeling for Personalized Neurorehabilitation Technologies. *IEEE Transactions on Biomedical Engineering* 2016, 63:879-893.
20. Farina D, Sartori M. Surface Electromyography for Man-Machine Interfacing in Rehabilitation Technologies. *Surface Electromyography: Physiology, Engineering and Applications* 2016, Pages 540-560.
21. Sartori M, Lloyd DG, Besier TF, Fernandez JW, Dario F. Electromyography-driven Modeling for Simulating Subject-Specific Movement at the Neuromusculoskeletal Level. *Electromyography: Physiology, Engineering, and Non-Invasive Applications* 2016, Pages 247-272.
22. Enoka RM. Biomechanics and neuroscience: A failure to communicate. *Exercise and Sport Sciences Reviews* 2004, 32:1-3.
23. van der Krogt MM, Bar-On L, Kindt T, Desloovere K, Harlaar J. Neuro-musculoskeletal simulation of instrumented contracture and spasticity assessment in children with cerebral palsy. *J Neuroeng Rehabil* 2016, 13:64.
24. Chang FM, Seidl AJ, Muthusamy K, Meininger AK, Carollo JJ. Effectiveness of instrumented gait analysis in children with cerebral palsy--comparison of outcomes. *J Pediatr Orthop.* 2006, 26:612-616.
25. Tugui RD, Antonescu D. Cerebral palsy gait, clinical importance. *Maedica (Buchar).* 2013, 8:388-393.
26. Filho MC, Yoshida R, Carvalho Wda S, Stein HE, Novo NF. Are the recommendations from three-dimensional gait analysis associated with better postoperative outcomes in patients with cerebral palsy? *Gait Posture.* 2008, 28:316-322. doi: 310.1016/j.gaitpost.2008.1001.1013. Epub 2008 Mar 1020.
27. Carty CP, Walsh HP, Gillett JG, Phillips T, Edwards JM, deLacy M, Boyd RN. The effect of femoral derotation osteotomy on transverse plane hip and pelvic kinematics in children with cerebral palsy: a systematic review and meta-analysis. *Gait Posture* 2014, 40:333-340.
28. Thomason P, Selber P, Graham HK. Single Event Multilevel Surgery in children with bilateral spastic cerebral palsy: a 5 year prospective cohort study. *Gait Posture.* 2013, 37:23-28. doi: 10.1016/j.gaitpost.2012.1005.1022. Epub 2012 Jul 1019.
29. Delp SL, Anderson FC, Arnold AS, Loan P, Habib A, John CT, Guendelman E, Thelen DG. OpenSim: open-source software to create and analyze dynamic simulations of movement. *IEEE Transactions on Biomedical Engineering* 2007, 54:1940-1950.

30. Damsgaard M, Rasmussen J, Christensen ST, Surma E, de Zee M. Analysis of musculoskeletal systems in the AnyBody Modeling System. *Simulation Modelling Practice and Theory* 2006, 14:1100-1111.
31. Riley PO, Franz J, Dicharry J, Kerrigan DC. Changes in hip joint muscle-tendon lengths with mode of locomotion. *Gait Posture* 2010, 31:279-283.
32. Arnold AS, Salinas S, Asakawa DJ, Delp SL. Accuracy of muscle moment arms estimated from MRI-based musculoskeletal models of the lower extremity. *Comput Aided Surg* 2000, 5:108-119.
33. Steele KM, van der Krogt MM, Schwartz MH, Delp SL. How much muscle strength is required to walk in a crouch gait? *J Biomech* 2012, 45:2564-2569.
34. Modenese L, Gopalakrishnan A, Phillips AT. Application of a falsification strategy to a musculoskeletal model of the lower limb and accuracy of the predicted hip contact force vector. *J Biomech* 2013, 46:1193-1200.
35. Steele KM, DeMers MS, Schwartz MH, Delp SL. Compressive tibiofemoral force during crouch gait. *Gait Posture* 2012, 35:556-560.
36. Graham DF, Carty CP, Lloyd DG, Lichtwark GA, Barrett RS. Muscle contributions to recovery from forward loss of balance by stepping. *J Biomech* 2014, 47:667-674.
37. Steele KM, Seth A, Hicks JL, Schwartz MH, Delp SL. Muscle contributions to vertical and fore-aft accelerations are altered in subjects with crouch gait. *Gait Posture* 2013, 38:86-91.
38. Arnold E, Ward S, Lieber R, Delp S. A Model of the Lower Limb for Analysis of Human Movement. *Annals of biomedical engineering* 2010, 38:269-279.
39. Delp SL, Loan JP, Hoy MG, Zajac FE, Topp EL, Rosen JM. An interactive graphics-based model of the lower extremity to study orthopaedic surgical procedures. *IEEE Transactions on Biomedical Engineering* 1990, 37:757-767.
40. Lloyd DG, Besier TF. An EMG-driven musculoskeletal model to estimate muscle forces and knee joint moments in vivo. *J Biomech* 2003, 36:765-776.
41. Modenese L, Phillips ATM, Bull AMJ. An open source lower limb model: Hip joint validation. *J Biomech* 2011, 44:2185-2193.
42. Brand RA, Crowninshield RD, Wittstock CE, Pedersen DR, Clark CR, van Krieken FM. A model of lower extremity muscular anatomy. *Journal of Biomechanical Engineering* 1982, 104:304-310.
43. Klein Horsman MD, Koopman HF, van der Helm FC, Prose LP, Veeger HE. Morphological muscle and joint parameters for musculoskeletal modelling of the lower extremity. *Clinical Biomechanics* 2007, 22:239-247.
44. Ward S, Eng C, Smallwood L, Lieber R. Are Current Measurements of Lower Extremity Muscle Architecture Accurate? *Clinical Orthopaedics and Related Research* 2009, 467:1074-1082.
45. Carbone V, Fluit R, Pellikaan P, van der Krogt MM, Janssen D, Damsgaard M, Vigneron L, Feilkas T, Koopman HFJM, Verdonschot N. Tlem 2.0–A Comprehensive Musculoskeletal Geometry Dataset For Subject-Specific Modeling Of Lower Extremity. *J Biomech* 2015.
46. Friederich JA, Brand RA. Muscle fiber architecture in the human lower limb. *J Biomech* 1990, 23:91-95.
47. Laracca E, Stewart C, Postans N, Roberts A. The effects of surgical lengthening of hamstring muscles in children with cerebral palsy--the consequences of pre-operative muscle length measurement. *Gait Posture* 2014, 39:847-851.
48. Scheys L, Desloovere K, Spaepen A, Suetens P, Jonkers I. Calculating gait kinematics using MR-based kinematic models. *Gait Posture* 2011, 33:158-164.
49. Scheys L, Desloovere K, Suetens P, Jonkers I. Level of subject-specific detail in musculoskeletal models affects hip moment arm length calculation during gait in pediatric subjects with increased femoral anteversion. *J Biomech* 2011, 44:1346-1353.
50. Davis RB, Õunpuu S, Tyburski D, Gage JR. A gait analysis data collection and reduction technique. *Human Movement Science* 1991, 10:575-587.

51. Kadaba MP, Ramakrishnan H, Wootten M. Measurement of lower extremity kinematics during level walking. *J Orthop Res* 1990, 8.
52. Davis R, Ounpuu S, Tyburski D, Gage J. A gait analysis data collection and reduction technique. *Human Movement Science* 1991, 10:575 - 587.
53. Arnold AS, Blemker SS, Delp SL. Evaluation of a deformable musculoskeletal model for estimating muscle-tendon lengths during crouch gait. *Ann Biomed Eng* 2001, 29:263-274.
54. Correa TA, Baker R, Graham HK, Pandy MG. Accuracy of generic musculoskeletal models in predicting the functional roles of muscles in human gait. *J Biomech* 2011, 44:2096-2105.
55. Lenaerts G, De Groote F, Demeulenaere B, Mulier M, Van der Perre G, Spaepen A, Jonkers I. Subject-specific hip geometry affects predicted hip joint contact forces during gait. *Journal of biomechanics* 2008, 41:1243-1252.
56. Bosmans L, Wesseling M, Desloovere K, Molenaers G, Scheys L, Jonkers I. Hip contact force in presence of aberrant bone geometry during normal and pathological gait. *J Orthop Res* 2014, 32:1406-1415.
57. Mudge AJ, Bau KV, Purcell LN, Wu JC, Axt MW, Selber P, Burns J. Normative reference values for lower limb joint range, bone torsion, and alignment in children aged 4-16 years. *J Pediatr Orthop B* 2014, 23:15-25.
58. Gage JR. Gait analysis. An essential tool in the treatment of cerebral palsy. *Clin Orthop Relat Res* 1993:126-134.
59. Hicks J, Arnold A, Anderson F, Schwartz M, Delp S. The effect of excessive tibial torsion on the capacity of muscles to extend the hip and knee during single-limb stance. *Gait Posture* 2007, 26:546-552.
60. Passmore E, Pandy MG, Graham HK, Sangeux M. Measuring Femoral Torsion In Vivo Using Freehand 3-D Ultrasound Imaging. *Ultrasound Med Biol* 2016, 42:619-623.
61. Passmore E, Sangeux M. Defining the medial-lateral axis of an anatomical femur coordinate system using freehand 3D ultrasound imaging. *Gait and Posture* in press.
62. Sangeux M, Eizenberg N, Graham HK. Measuring femoral neck anteversion - Validation of a technique based on 3D freehand ultrasound. *22nd Annual Meeting of the European Society for Movement Analysis in Adults and Children* 2013.
63. Oberhofer K, Mithraratne K, Stott N, Anderson I. Anatomically-based musculoskeletal modeling: prediction and validation of muscle deformation during walking. *The Visual Computer* 2009, 25:843-851.
64. Valente G, Pitto L, Testi D, Seth A, Delp SL, Stagni R, Viceconti M, Taddei F. Are Subject-Specific Musculoskeletal Models Robust to the Uncertainties in Parameter Identification? *PLoS One* 2014, 9:e112625.
65. Kainz H, Modenese L, Lloyd DG, Maine S, Walsh HP, Carty CP. Joint kinematic calculation based on clinical direct kinematic versus inverse kinematic gait models. *J Biomech* 2016, 49:1658-1669.
66. Brito da Luz S, Saxby DJ, Modenese L, Mills PM, Beck B, Besier TF, Lloyd DG. COMPLETE OPENSIM SUBJECT-SPECIFIC LOWER LIMB JOINT-SKELETAL MRI-BASED MODEL. *XXV Congress of the International Society of Biomechanics* 2015.
67. Heinrich SD, MacEwen GD, Zembo MM. Hip dysplasia, subluxation, and dislocation in cerebral palsy: an arthrographic analysis. *J Pediatr Orthop* 1991, 11:488-493.
68. Martelli S, Valente G, Viceconti M, Taddei F. Sensitivity of a subject-specific musculoskeletal model to the uncertainties on the joint axes location. *Computer Methods in Biomechanics and Biomedical Engineering* 2014:1-9.
69. Yin L, Chen K, Guo L, Cheng L, Wang F, Yang L. Identifying the Functional Flexion-extension Axis of the Knee: An In-Vivo Kinematics Study. *PloS one* 2015, 10:e0128877.
70. Prinold JI, Mazzà C, Di Marco R, Hannah I, Malattia C, Magni-Manzoni S, Petrarca M, Ronchetti A, Tanturri de Horatio L, van Dijkhuizen EHP, et al. A Patient-Specific Foot Model

for the Estimate of Ankle Joint Forces in Patients with Juvenile Idiopathic Arthritis. *Annals of biomedical engineering* 2016, 44:247-257.
71. Siegler S, Toy J, Seale D, Pedowitz D. The Clinical Biomechanics Award 2013--presented by the International Society of Biomechanics: New observations on the morphology of the talar dome and its relationship to ankle kinematics. *Clinical Biomechanics* 2014, 29:1-6.
72. Parr WCH, Chatterjee HJ, Soligo C. Calculating the axes of rotation for the subtalar and talocrural joint using 3D bone reconstructions. *J Biomech* 2012, 45:1103-1107.
73. Parenti-Castelli V, Sancisi N. Synthesis of Spatial Mechanisms to Model Human Joints. In: *21st Century Kinematics*: Springer; 2013, 49-84.
74. Gasparutto X, Sancisi N, Jacquelin E, Parenti-Castelli V, Dumas R. Validation of a multi-body optimization with knee kinematic models including ligament constraints. *J Biomech* 2015, 48:1141-1146.
75. Brito da Luz S, Modenese L, Mills PM, Beck B, Sancisi N, Besier TF, Lloyd DG. MRI BASED PARALLEL MECHANISMS TO MODEL SUBJECT-SPECIFIC KNEE KINEMATICS. *XXV Congress of the International Society of Biomechanics* 2015.
76. Clément J, Dumas R, Hagemeister N, de Guise JA. Soft tissue artifact compensation in knee kinematics by multi-body optimization: Performance of subject-specific knee joint models. *J Biomech* 2015, 48:3796-3802.
77. Passmore E, Pandy MG, Graham HK, Sangeux M. Measuring Femoral Torsion in Vivo Using Freehand 3-D Ultrasound Imaging. *Ultrasound Med Biol* 2015.
78. Duprey S, Cheze L, Dumas R. Influence of joint constraints on lower limb kinematics estimation from skin markers using global optimization. *J Biomech* 2010, 43:2858-2862.
79. Lu TW, O'Connor JJ. Bone position estimation from skin marker co-ordinates using global optimisation with joint constraints. *J Biomech* 1999, 32:129-134.
80. Andersen MS, Damsgaard M, Rasmussen J. Kinematic analysis of over-determinate biomechanical systems. *Computer Methods in Biomechanics and Biomedical Engineering* 2009, 12:371-384.
81. Dempster WT. Space requirements of the seated operator. *Tech. Rep. WADC 55-159* 1955.
82. de Leva P. Adjustments to Zatsiorsky-Seluyanov's segment inertia parameters. *J Biomech* 1996, 29:1223-1230.
83. Bresler B, Frankel JP. The forces and moments in the leg during level walking. *Transactions of the American Society of Mechanical Engineers* 1950, 72:27-36.
84. Dumas R, Aissaoui R, Mitton D, Skalli W, de Guise JA. Personalized body segment parameters from biplanar low-dose radiography. *IEEE Transactions on Biomedical Engineering* 2005, 52:1756-1763.
85. White D, Woodard H, Hammond S. Average soft-tissue and bone models for use in radiation dosimetry. *The British journal of radiology* 1987, 60:907-913.
86. Damsgaard M, Rasmussen J, Christensen SrTr, Surma E, de Zee M. Analysis of musculoskeletal systems in the AnyBody Modeling System. *Simulation Modelling Practice and Theory* 2006, 14:1100-1111.
87. Delp SL, Loan JP, Hoy MG, Zajac FE, Topp EL, Rosen JM. An Interactive Graphics-Based Model of the Lower Extremity to Study Orthopaedic Surgical Procedures. *IEEE Transactions on Biomedical Engineering* 1990, 37:757-767.
88. Oberhofer K, Stott NS, Mithraratne K, Anderson Ia. Subject-specific modelling of lower limb muscles in children with cerebral palsy. *Clinical Biomechanics* 2010, 25:88-94.
89. Zhang J, Hislop-Jambrich J, Besier TF. Predictive statistical models of baseline variations in 3-D femoral cortex morphology. *Medical Engineering & Physics* 2016, In Press.
90. Morrell DS, Pearson JM, Sauser DD. Progressive bone and joint abnormalities of the spine and lower extremities in cerebral palsy. *Radiographics : a review publication of the Radiological Society of North America, Inc* 2002, 22:257-268.

91. Mergler S, Evenhuis HM, Boot AM, De Man SA, Bindels-De Heus KGCB, Huijbers WAR, Penning C. Epidemiology of low bone mineral density and fractures in children with severe cerebral palsy: a systematic review. *Dev Med Child Neurol* 2009, 51:773-778.
92. Stevenson RD, Conaway M, Barrington JW, Cuthill SL, Worley G, Henderson RC. Fracture rate in children with cerebral palsy. *Pediatric Rehabilitation* 2009, 9:396-403.
93. Rosenbaum P, Paneth N, Leviton A, Goldstein M, Bax M, Damiano D, Dan B, Jacobsson B. A report: the definition and classification of cerebral palsy April 2006. *Developmental medicine and child neurology. Supplement* 2007, 109:8-14.
94. Zhang J, Malcolm D, Hislop-Jambrich J, Thomas CDL, Nielsen PMF. An Anatomical Region-based Statistical Shape Model of the Human Femur. *Computer Methods in Biomechanics and Biomedical Engineering: Imaging & Visualization* 2014, 2:176-185.
95. Bryan R, Mohan PS, Hopkins A, Galloway F, Taylor M, Nair PB. Statistical modelling of the whole human femur incorporating geometric and material properties. *Medical Engineering & Physics* 2010, 32:57-65.
96. Harris M, Datar M, Jurrus E, Peters C. Statistical Shape Modeling of Cam-Type Femoroacetabular Impingement. *Journal of Orthopaedic Research* 2013, 32:1620-1626.
97. Schneider MTY, Zhang J, Crisco JJ, Weiss APC, Ladd AL, Nielsen P, Besier T. Men and women have similarly shaped carpometacarpal joint bones. *J Biomech* 2015, 48:3420-3426.
98. Zhang J, Sorby H, Clement J, Thomas CDL, Hunter P, Nielsen P, Lloyd D, Taylor M, Besier T. The MAP Client: User-Friendly Musculoskeletal Modelling Workflows. *Biomedical Simulation* 2014. Vol. 8789, Pages 182-192.
99. Anderson AE, Ellis BJ, Maas SA, Weiss JA. Effects of idealized joint geometry on finite element predictions of cartilage contact stresses in the hip. *J Biomech* 2010, 43:1351-1357.
100. Fernandez J, Zhang J, Heidlauf T, Sartori M, Besier T, Röhrle O, Lloyd D. Multiscale musculoskeletal modelling, data–model fusion and electromyography-informed modelling. *Interface Focus* 2016, 6:20150084.
101. Barrett RS, Lichtwark GA. Gross muscle morphology and structure in spastic cerebral palsy: a systematic review. *Dev Med Child Neurol* 2010, 52:794-804.
102. Gormley ME, Gaebler-Spira D, Delgado MR. Use of botulinum toxin type A in pediatric patients with cerebral palsy: a three-center retrospective chart review. *Journal of child neurology* 2001, 16:113-118.
103. Smith LR, Lee KS, Ward SR, Chambers HG, Lieber RL. Hamstring contractures in children with spastic cerebral palsy result from a stiffer extracellular matrix and increased in vivo sarcomere length. *The Journal of physiology* 2011, 589:2625-2639.
104. Handsfield GG, Meyer CH, Abel MF, Blemker SS. Heterogeneity of muscle sizes in the lower limbs of children with cerebral palsy. *Muscle and Nerve* 2015.
105. Handsfield GG, Meyer CH, Hart JM, Abel MF, Blemker SS. Relationships of 35 lower limb muscles to height and body mass quantified using MRI. *J Biomech* 2014, 47:631-638.
106. Holzbaur KR, Murray WM, Gold GE, Delp SL. Upper limb muscle volumes in adult subjects. *J Biomech* 2007, 40:742-749.
107. Noble JJ, Fry NR, Lewis AP, Keevil SF, Gough M, Shortland AP. Lower limb muscle volumes in bilateral spastic cerebral palsy. *Brain & development* 2014, 36:294-300.
108. Arnold * aS, Delp SL. Computer modeling of gait abnormalities in cerebral palsy: application to treatment planning. *Theoretical Issues in Ergonomics Science* 2005, 6:305-312.
109. Delp SL, Arnold AS, Speers RA, Moore CA. Hamstrings and psoas lengths during normal and crouch gait: Implications for muscle-tendon surgery. *Journal of Orthopaedic Research* 1996. Vol. 14, Pages 144-151.
110. Fernandez JW, Mithraratne P, Thrupp SF, Tawhai MH, Hunter PJ. Anatomically based geometric modelling of the musculo-skeletal system and other organs. *Biomech Model Mechanobiol* 2004, 2:139-155.

111. Ackerman MJ. The Visible Human Project: a resource for anatomical visualization. *Stud Health Technol Inform* 1998, 52 Pt 2:1030-1032.
112. Bradley CP, Pullan AJ, Hunter PJ. Geometric modeling of the human torso using cubic hermite elements. *Ann Biomed Eng* 1997, 25:96-111.
113. Fernandez JW, Hunter PJ. An anatomically based patient-specific finite element model of patella articulation: towards a diagnostic tool. *Biomech Model Mechanobiol* 2005, 4:20-38.
114. Blemker SS, Delp SL. Three-dimensional representation of complex muscle architectures and geometries. *Ann Biomed Eng* 2005, 33:661-673.
115. Lemos RR, Epstein M, Herzog W. Modeling of skeletal muscle: the influence of tendon and aponeuroses compliance on the force-length relationship. *Med Biol Eng Comput* 2008, 46:23-32.
116. Fernandez JW, Ho A, Walt S, Anderson IA, Hunter PJ. A cerebral palsy assessment tool using anatomically based geometries and free-form deformation. *Biomech Model Mechanobiol* 2005, 4:39-56.
117. Lieber RL, Friden J. Functional and clinical significance of skeletal muscle architecture. *Muscle and Nerve* 2000, 23:1647-1666.
118. Bottos M, Feliciangeli A, Sciuto L, Gericke C, Vianello A. Functional status of adults with cerebral palsy and implications for treatment of children. *Developmental Medicine & Child Neurology* 2001, 43:516-528.
119. Barber L, Hastings-Ison T, Baker R, Barrett R, Lichtwark G. Medial gastrocnemius muscle volume and fascicle length in children aged 2 to 5 years with cerebral palsy. *Developmental Medicine and Child Neurology* 2011, 53:543-548.
120. Barber L, Barrett R, Lichtwark G. Medial gastrocnemius muscle fascicle active torque-length and Achilles tendon properties in young adults with spastic cerebral palsy. *J Biomech* 2012, 45:2526-2530.
121. Barber L, Read F, Lovatt Stern J, Lichtwark G, Boyd RN. Medial gastrocnemius muscle volume in ambulant children with unilateral and bilateral cerebral palsy aged 2 to 9 years. *Developmental Medicine and Child Neurology* 2016, 58:485-491.
122. Noble JJ, Charles-Edwards GD, Keevil SF, Lewis AP, Gough M, Shortland AP. Intramuscular fat in ambulant young adults with bilateral spastic cerebral palsy. *BMC Musculoskeletal Disorders* 2014, 15:236.
123. Barber LA, Read F, Lovatt Stern J, Lichtwark G, Boyd RN. Medial gastrocnemius muscle volume in ambulant children with unilateral and bilateral cerebral palsy aged 2 to 9 years. *Dev Med Child Neurol* 2016, 58:1146-1152.
124. Barber L, Hastings-Ison T, Baker R, Graham HK, Barrett R, Lichtwark G. The effects of Botulinum toxin injection frequency on calf muscle growth in young children with spastic cerebral palsy: A 12 month prospective study. *Journal of Children's Orthopaedics* 2013, 7:425-433.
125. Eek MN, Beckung E. Walking ability is related to muscle strength in children with cerebral palsy. *Gait Posture* 2008, 28:366-371.
126. Perry J, Hoffer MM, Giovan P, Antonelli D, Greenberg R. Gait analysis of the triceps surae in cerebral palsy. A preoperative and postoperative clinical and electromyographic study. *Journal of Bone and Joint Surgery. American Volume* 1974, 56:511-520.
127. Elder GC, Kirk J, Stewart G, Cook K, Weir D, Marshall A, Leahey L. Contributing factors to muscle weakness in children with cerebral palsy. *Developmental Medicine and Child Neurology* 2003, 45:542-550.
128. Fry NR, Gough M, McNee AE, Shortland AP. Changes in the volume and length of the medial gastrocnemius after surgical recession in children with spastic diplegic cerebral palsy. *Journal of Pediatric Orthopaedics* 2007, 27:769-774.

129. Gao F, Grant TH, Roth EJ, Zhang LQ. Changes in passive mechanical properties of the gastrocnemius muscle at the muscle fascicle and joint levels in stroke survivors. *Archives of Physical Medicine and Rehabilitation* 2009, 90:819-826.
130. Zhao H, Ren Y, Wu YN, Liu SQ, Zhang LQ. Ultrasonic evaluations of Achilles tendon mechanical properties poststroke. *Journal of Applied Physiology* 2009, 106:843-849.
131. Mohagheghi AA, Khan T, Meadows TH, Giannikas K, Baltzopoulos V, Maganaris CN. In vivo gastrocnemius muscle fascicle length in children with and without diplegic cerebral palsy. *Developmental Medicine and Child Neurology* 2008, 50:44-50.
132. Moreau NG, Teefey SA, Damiano DL. In vivo muscle architecture and size of the rectus femoris and vastus lateralis in children and adolescents with cerebral palsy. *Developmental Medicine and Child Neurology* 2009, 51:800-806.
133. Malaiya R, McNee AE, Fry NR, Eve LC, Gough M, Shortland AP. The morphology of the medial gastrocnemius in typically developing children and children with spastic hemiplegic cerebral palsy. *Journal of Electromyography and Kinesiology* 2007, 17:657-663.
134. Shortland AP, Harris CA, Gough M, Robinson RO. Architecture of the medial gastrocnemius in children with spastic diplegia. *Developmental Medicine and Child Neurology* 2002, 44:158-163.
135. Lichtwark GA, Bougoulias K, Wilson AM. Muscle fascicle and series elastic element length changes along the length of the human gastrocnemius during walking and running. *Journal of Biomechanics* 2007, 40:157-164.
136. Barber L, Barrett R, Lichtwark G. Passive mechanical properties of the medial gastrocnemius muscle in young adults with cerebral palsy. *Journal of Biomechanics* 2011, 44:2496-2500.
137. Gao F, Zhao H, Gaebler-Spira D, Zhang LQ. In vivo evaluations of morphologic changes of gastrocnemius muscle fascicles and achilles tendon in children with cerebral palsy. *American Journal of Physical Medicine and Rehabilitation* 2011, 90:364-371.
138. Theis N, Korff T, Kairon H, Mohagheghi AA. Does acute passive stretching increase muscle length in children with cerebral palsy? *Clinical Biomechanics* 2013, 28:1061-1067.
139. Wren TA, Cheatwood AP, Rethlefsen SA, Hara R, Perez FJ, Kay RM. Achilles tendon length and medial gastrocnemius architecture in children with cerebral palsy and equinus gait. *Journal of Pediatric Orthopedics* 2010, 30:479-484.
140. Zhao H, Wu Y, Hwang M, Ren Y, Gao F, Gaebler-Spira D, Zhang L. Changes of calf muscle-tendon biomechanical properties induced by passive stretching and active movement training in children with cerebral palsy. *Journal of Applied Physiology* 2011, 111:435-442.
141. Kalsi G, Fry NR, Shortland AP. Gastrocnemius muscle-tendon interaction during walking in typically-developing adults and children, and in children with spastic cerebral palsy. *J Biomech* 2016.
142. Hosl M, Bohm H, Arampatzis A, Keymer A, Doderlein L. Contractile behavior of the medial gastrocnemius in children with bilateral spastic cerebral palsy during forward, uphill and backward-downhill gait. *Clin Biomech (Bristol, Avon)* 2016, 36:32-39.
143. Riad J, Haglund-Akerlind Y, Miller F. Power generation in children with spastic hemiplegic cerebral palsy. *Gait and Posture* 2008, 27:641-647.
144. Verschuren O, Maltais DB, Douma-van Riet D, Kruitwagen C, Ketelaar M. Anaerobic Performance in Children With Cerebral Palsy Compared to Children With Typical Development. *Pediatr Phys Ther* 2013.
145. Ross SA, Engsberg JR. Relationships between spasticity, strength, gait, and the GMFM-66 in persons with spastic diplegia cerebral palsy. *Archives of Physical Medicine and Rehabilitation* 2007, 88:1114-1120.
146. Farina D, Rehbaum H, Holobar A, Vujaklija I, Jiang N, Hofer C, Salminger S, Van Vliet HW, Aszmann OC. Noninvasive, accurate assessment of the behavior of representative populations of motor units in targeted reinnervated muscles. *IEEE Transactions on Neural Systems and Rehabilitation Engineering* 2014, 22:810-819.

147. Sartori M, Reggiani M, Farina D, Lloyd DG. EMG-driven forward-dynamic estimation of muscle force and joint moment about multiple degrees of freedom in the human lower extremity. *PLoS ONE* 2012, 7:1-11.
148. Bizzi E, Cheung VCK, d'Avella a, Saltiel P, Tresch M. Combining modules for movement. *Brain research reviews* 2008, 57:125-133.
149. Enoka RM. Neuromechanics of Human Movement. 2008:1-560.
150. Pandy MG, Andriacchi TP. Muscle and joint function in human locomotion. *Annual review of biomedical engineering* 2010, 12:401-433.
151. Seth A, Pandy MG. A neuromusculoskeletal tracking method for estimating individual muscle forces in human movement. *Journal of Biomechanics* 2007, 40:356-366.
152. Anderson FC, Pandy MG. Dynamic optimization of human walking. *Journal of Biomechanical Engineering* 2001, 123:381-390.
153. Wang JM, Hamner SR, Delp SL, Koltun V. Optimizing locomotion controllers using biologically-based actuators and objectives. *ACM Transactions on Graphics* 2012, 31:1-11.
154. Sartori M, Farina D, Lloyd DG. Hybrid neuromusculoskeletal modeling to best track joint moments using a balance between muscle excitations derived from electromyograms and optimization. *Journal of Biomechanics* 2014, 47:3613-3621.
155. Pizzolato C, Lloyd DG, Sartori M, Ceseracciu E, Besier TF, Fregly BJ, Reggiani M. CEINMS: A toolbox to investigate the influence of different neural control solutions on the prediction of muscle excitation and joint moments during dynamic motor tasks. *Journal of Biomechanics* 2015.
156. Sartori M, Reggiani M, Pagello E, Lloyd DG. Modeling the human knee for assistive technologies. *IEEE transactions on bio-medical engineering* 2012, 59:2642-2649.
157. Sartori M, Gizzi L, Lloyd DG, Farina D. A musculoskeletal model of human locomotion driven by a low dimensional set of impulsive excitation primitives. *Frontiers in Computational Neuroscience* 2013, 7:79.
158. Lee DD, Seung HS. Learning the parts of objects by non-negative matrix factorization. *Nature* 1999, 401:788-791.
159. Sartori M, Reggiani M, van den Bogert AJ, Lloyd DG. Estimation of musculotendon kinematics in large musculoskeletal models using multidimensional B-splines. *Journal of Biomechanics* 2012, 45:595-601.
160. Schaffelhofer S, Sartori M, Scherberger H, Farina D. Musculoskeletal Representation of a Large Repertoire of Hand Grasping Actions in Primates. *IEEE Transactions on Neural Systems and Rehabilitation Engineering* 2015, 23:1-11.
161. Gonzalez-Vargas J, Sartori M, Dosen S, Torricelli D, Pons JL, Farina D. A predictive model of muscle excitations based on muscle modularity for a large repertoire of human locomotion conditions. *Frontiers in Computational Neuroscience* 2015, 9:1-14.
162. Heintz S, Gutierrez-farewik EM. Static optimization of muscle forces during gait in comparison to EMG-to-force processing approach. 2007, 26:279-288.
163. Gerus P, Sartori M, Besier TF, Fregly BJ, Delp SL, Banks Sa, Pandy MG, D'Lima DD, Lloyd DG. Subject-specific knee joint geometry improves predictions of medial tibiofemoral contact forces. *Journal of Biomechanics* 2013, 46:2778-2786.
164. Sartori M, Maculan M, Pizzolato C, Reggiani M, Farina D. Modeling and Simulating the Neuromuscular Mechanisms regulating Ankle and Knee Joint Stiffness during Human Locomotion. *Journal of Neurophysiology* 2015, 114:2509-2527.
165. Kinney AL, Besier TF, D'Lima DD, Fregly BJ. Update on Grand Challenge Competition to Predict in Vivo Knee Loads. *Journal of Biomechanical Engineering* 2013, 135:21012.
166. Fregly BJ, Besier TF, Lloyd DG, Delp SL, Banks SA, Pandy MG, D'Lima DD. Grand challenge competition to predict in vivo knee loads. *Journal of orthopaedic research : official publication of the Orthopaedic Research Society* 2012, 30:503-513.

167. Fernandez J, Sartori M, Lloyd D, Munro J, Shim V. Bone remodelling in the natural acetabulum is influenced by muscle force-induced bone stress. *International Journal for Numerical Methods in Biomedical Engineering* 2014, 30:28-41.
168. Navarro X, Krueger TB, Lago N, Micera S, Stieglitz T, Dario P. A Critical Review of Interfaces with the Peripheral Nervous System for the Control of Neuroprotheses and Hybrid Bionic Systems. *J Peripher Nerv Syst* 2005, 10:229-258.
169. Farina D, Aszmann O. Bionic Limbs: Clinical Reality and Academic Promises. *Science Translational Medicine* 2014, 6:257ps212.
170. Hicks JL, Uchida TK, Seth a, Rajagopal a, Delp S. Is my model good enough? Best practices for verification and validation of musculoskeletal models and simulations of human movement. *Journal of Biomechanical Engineering* 2014, 137.
171. Oberhofer K, Stott NS, Mithraratne K, Anderson IA. Subject-specific modelling of lower limb muscles in children with cerebral palsy. *Clinical Biomechanics* 2010, 25:88-94.
172. Barber L, Barrett R, Lichtwark G. Passive muscle mechanical properties of the medial gastrocnemius in young adults with spastic cerebral palsy. *J Biomech* 2011, 44:2496-2500.
173. Modenese L, Ceseracciu E, Reggiani M, Lloyd DG. Estimation of musculotendon parameters for scaled and subject specific musculoskeletal models using an optimization technique. *J Biomech* 2016, 49:141-148.
174. Winby CR, Lloyd DG, Kirk TB. Evaluation of different analytical methods for subject-specific scaling of musculotendon parameters. *J Biomech* 2008, 41:1682-1688.
175. Buchanan TS, Lloyd DG, Manal K, Besier TF. Neuromusculoskeletal modeling: estimation of muscle forces and joint moments and movements from measurements of neural command. *Journal of applied Biomechanics* 2004, 20:367.
176. Garner BA, Pandy MG. Estimation of Musculotendon Properties in the Human Upper Limb. *Annals of biomedical engineering* 2003, 31:207-220.
177. Zajac FE. Muscle and tendon: properties, models, scaling, and application to biomechanics and motor control. *Critical Reviews in Biomedical Engineering* 1989, 17:359-411.
178. Phillips ATM, Villette CC, Modenese L. Femoral bone mesoscale structural architecture prediction using musculoskeletal and finite element modelling. *International Biomechanics* 2015, 2:43-61.
179. van Arkel RJ, Modenese L, Phillips A, Jeffers JR. Hip Abduction Can Prevent Posterior Edge Loading of Hip Replacements. *Journal of Orthopaedic Research* 2013, 31:1172-1179.
180. Modenese L, Phillips A. Prediction of hip contact forces and muscle activations during walking at different speeds. *Multibody System Dynamics* 2012, 28:157-168.
181. Geraldes DM, Modenese L, Phillips A. Consideration of multiple load cases is critical in modelling orthotropic bone adaptation in the femur. *Biomechanics and modeling in mechanobiology* 2016, 15.:1029-1042.
182. Martelli S, Kersh ME, Schache AG, Pandy MG. Strain energy in the femoral neck during exercise. *J Biomech* 2014, 47:1784-1791.
183. Menegaldo LL, de Toledo Fleury A, Weber HI. Moment arms and musculotendon lengths estimation for a three-dimensional lower-limb model. *Journal of Biomechanics* 2004, 37:1447-1453.
184. Eskinazi I, Fregly BJ. Surrogate modeling of deformable joint contact using artificial neural networks. *Medical Engineering & Physics* 2015, 37:885-891.